Inflammatory Diseases of the Skin

4

Ximena Wortsman, Laura Carreño, and Claudia Morales

An insight into the world of sonography in psoriasis, morphea, lupus, dermatomyositis, and hidradenitis suppurativa, among others

Contents

4.1 Introduction

This chapter comprises several entities from different origins that can vary from trauma to viral infections or autoimmune diseases. Sonography has been proved useful for unmasking the anatomical changes that affect the skin layers and deeper structures during the inflammatory phases and also may show variable degrees of activity such as active, inactive, or atrophic stages in these conditions. In this chapter we will review the most common cutaneous inflammatory entities that may undergo ultrasonography.

The sonographer usually plays an active role in the assessment of the staging of inflammatory entities, sometimes having to extend the examination to other regions initially not previously requested by the referring physician. Thus, dealing with inflammatory conditions may also imply examining single or multiple lesions during the course of the same examination; therefore, baseline knowledge of the common sites of involvement in some of the entities may facilitate the process. Additionally, details such as sequential lighting of the examination room should be considered to properly place the probe when dealing with multiple locations.

4.2 Pathology

4.2.1 Hematomas-Seromas

Fluid collections secondary to trauma comprise one of the common causes of ultrasound requests in the soft tissues. The difference between hematomas and seromas is that hematomas contain a high presence of red blood cells, blot clots, and inflammatory cells in the acute phase that also show fibrin, granulation tissue, and debris in the late phases. In contrast, seromas (also called lymphoceles) are mainly composed of clear serous lymph fluid usually generated by leaks in the lymphatic network. Patients presenting with hemophilia, Ehler-Danlos syndrome, and sickle cell anemia may also easily have hematomas in the soft tissues. Thus, fluid hematic

X. Wortsman, MD (✉)
Department of Radiology and Dermatology,
Institute for Diagnostic Imaging
and Research of the Skin and Soft Tissues,
Clinica Servet, University of Chile, Faculty of Medicine,
Almirante Pastene 150, Providencia, Santiago, Chile
e-mail: xwo@tie.cl, xworts@yahoo.com, www.sonoskin.com

L. Carreño, MD • C. Morales, MD
Department of Pathology,
Dermopathology Section,
Hospital Clinico Universidad de Chile, Faculty of Medicine,
University of Chile, Santiago, Chile
e-mail: lcarrenotoro@gmail.com;
claudiamohuber@gmail.com

X. Wortsman, G.B.E. Jemec (eds.), *Dermatologic Ultrasound with Clinical and Histologic Correlations*,
DOI 10.1007/978-1-4614-7184-4_4,

collections are frequently found in the cutaneous layers and can vary in their sonographic representation according to the main composition, phase of involvement, and presence of liquefaction that could also show a mixed pattern (sero-hematic collections). Hematomas may commonly present on sonography as anechoic collections that can turn to hypoechoic or heterogeneous within days or weeks. Seromas usually present as anechoic clean collections as a result of their serous component. At the beginning the fluid collections are usually compressible with the probe and at late stages, compression is hard to perform because the fluid has been replaced by fibrous tissue and scarring components. The size of the collection also varies over a short period of time (days) and the sonographic follow up could be an objective way to confirm the regression of the hematoma. The latter fact could be important when dealing with hemorrhagic soft-tissue tumors that can occasionally mimic hematomas, but these entities usually do not significantly regress over days. Hemorrhagic tumors commonly show a mixed echogenicity with hypoechoic-anechoic or heterogeneous echogenicity, and they present low or absent capability of compression with the probe. Color Doppler can show peripherical hypervascularity in hematomas at the initial stages and hypovascularity at the late phases [1–5] (Fig. 4.1).

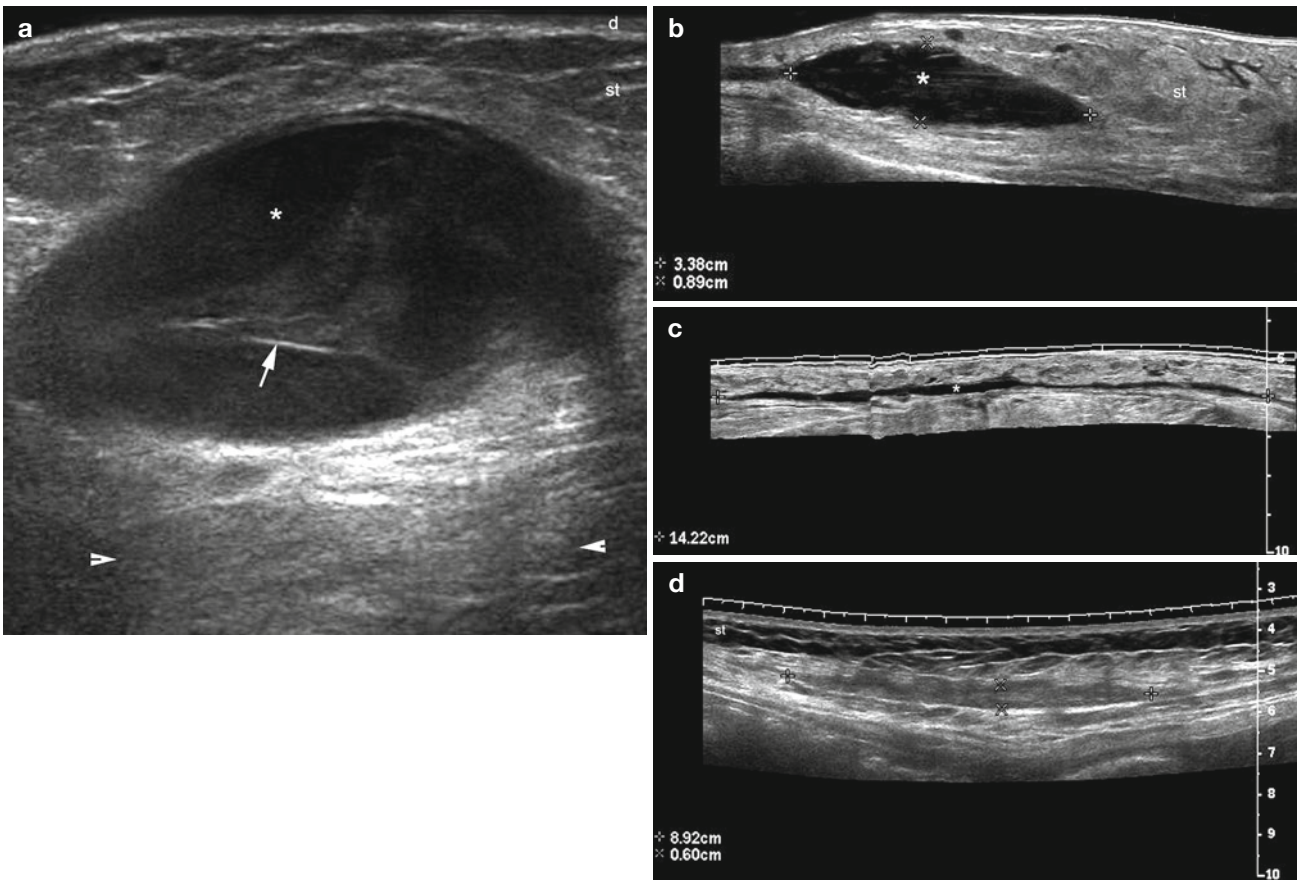

Fig. 4.1 (**a**–**d**) Hematomas. Sonographic appearances of hematic fluid collections (* and between markers) going from large (**a**, **b**) to laminar deposits (**c**, **d**). Notice the posterior acoustic reinforcement (*arrowheads*) and the internal septation (*arrow*) clearly depicted in (a). *Abbreviations*: *d* dermis, *st* subcutaneous tissue

4.2.2 Abscesses

Abscesses imply the presence of infection and/or pus within a fluid collection. Common causes of these organized collections are hematomas, ruptured epidermal cysts, inflamed pilonidal cysts, etc. Skin and soft-tissue infections are also the most common cause for hospital admission of injection drug users [6]. Abscesses present on ultrasound as distended anechoic or heterogeneous fluid collections, usually with multiple echoes or debris. They sometimes present anechoic communicating tracts to superficial (e.g., epidermal or subepidermal) or deep (e.g., muscular or articular) layers. Color Doppler usually demonstrates increase blood flow predominantly in the periphery of the collection [7]. Ultrasound-guided needle aspiration can be a useful technique for the identification of causative pathogens, and good results could be expected with ultrasound-guided gun biopsy culture from lesions without fluid collection [8] (Figs. 4.2 and 4.3).

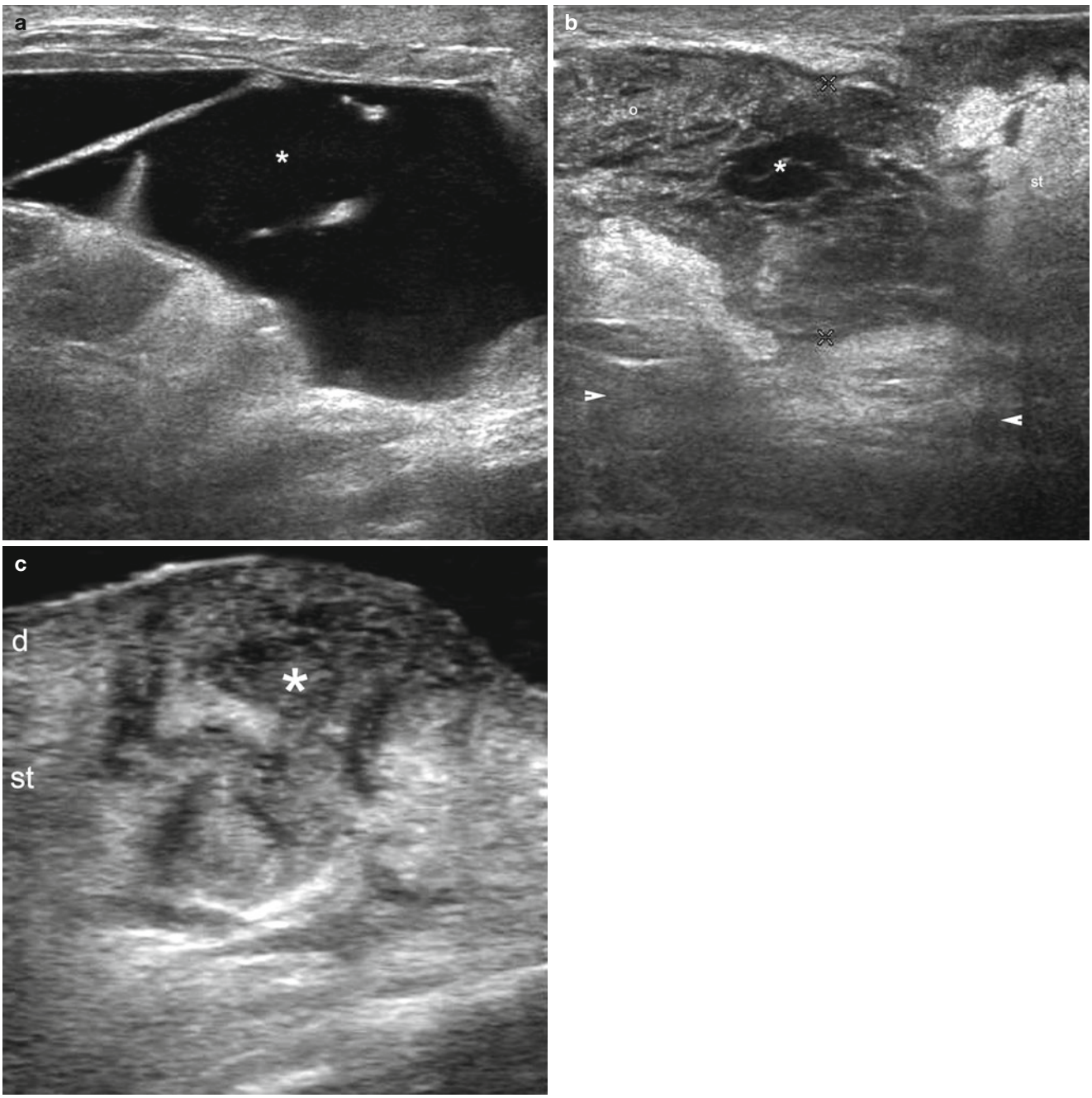

Fig. 4.2 (**a**–**c**) Abscesses. Variable sonographic appearances of cutaneous abscesses. (**a**) Large abscess that presents anechogenicity and prominent septa within the collection (*). (**b**) Abscess that shows heterogeneous echogenicity (o and *, hypoechoic and anechoic areas, respectively). A posterior acoustic reinforcement artifact (*arrowhead*) is also demonstrated. (**c**) There is an ill-defined fluid collection mostly hypoechoic and heterogeneous located in the dermis and subcutaneous tissue. *Abbreviations*: *d* dermis, *st* subcutaneous tissue

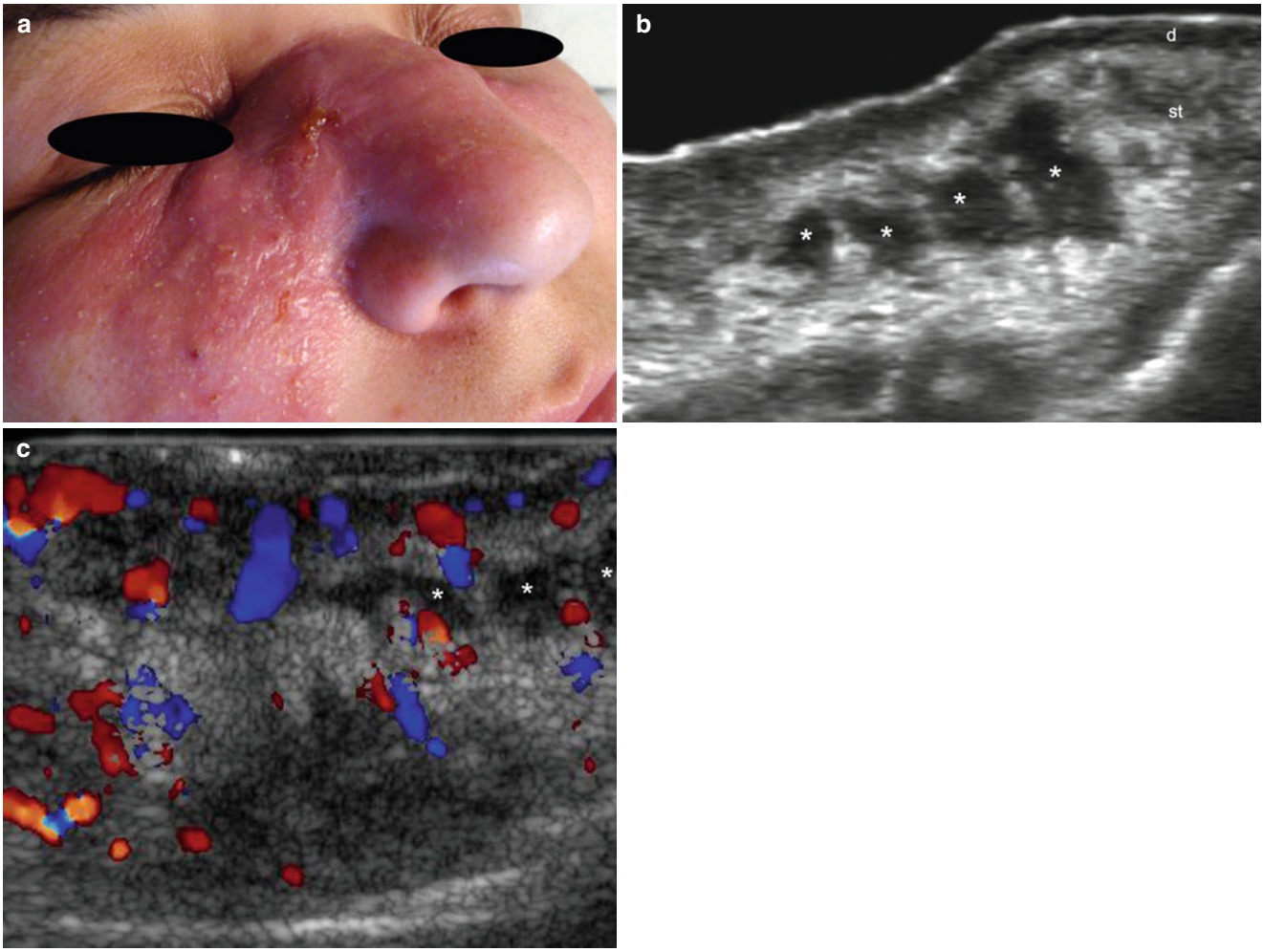

Fig. 4.3 (**a**–**c**) Multiple cutaneous abcesses. (**a**) Clinical lesion shows erythema and swelling at the right cheek. (**b**) Gray scale (transverse view) shows multiple round and oval shaped hypoechoic fluid collections (*) and increased echogenicity of the surrounding subcutaneous tissue. (**c**) Color Doppler (transverse view) demonstrates increased vascularity in the periphery of the collections (*). *Abbreviations*: *d* dermis, *st* subcutaneous tissue

4.2.3 Edema

The retention of fluid within the skin layers can be caused by various entities from trauma to inflammatory diseases. The venous and/or lymphatic systems usually fail to remove the excess of fluid that becomes stuck between the fatty lobules of the subcutaneous tissue. The incompetence of the lymphatic system is called lymphedema and differs from lipoedema, the latter being a different concept that implies an accumulation of fat abnormally distributed in the lower limbs [9]. Ultrasound has been reported to support the assessment of the changes in the thickness of the skin layers in post-thrombotic syndrome and the monitoring of the compression therapy in chronic venous disease [10]. Impairment of cutaneous microcirculation is a major predisposing factor in inflammation and ulceration in patients with chronic venous insufficiency (CVI). Increase of capillary filtration rate predisposes to the formation of edema. Local lymphedema is a complication of CVI and is often underdiagnosed [11]. On sonography, edema usually appears as anechoic fluid between the lobules of the subcutaneous tissue. In cases with lymphedema there is thickening of all the cutaneous layers, hypoechogenicity of the dermis, and increased echogenicity of the subcutaneous tissue in addition to the anechoic fluid between the fatty lobules of the hypodermis (Figs. 4.4 and 4.5).

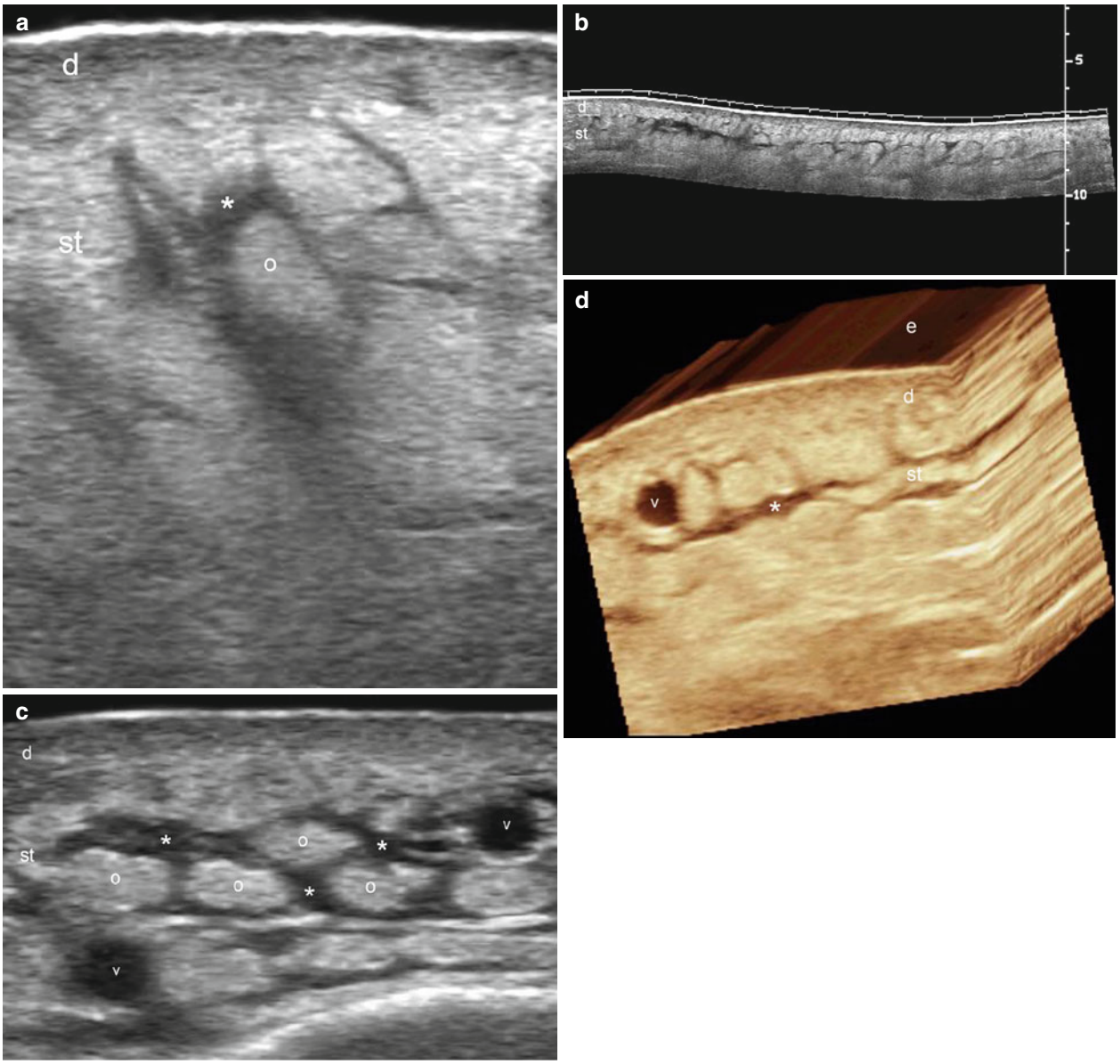

Fig. 4.4 (**a**–**d**) Cutaneous edema. Variable sonographic representations of cutaneous edema that show thickening and decreased echogenicity of the dermis and increased echogenicity of the fatty lobules (o) of the subcutaneous tissue. Notice the hypoechoic or anechoic fluid (*) in between the fatty lobules. Blurring of the borders of the lobules can be also detected (**a**, **b**). In (**c**), there is fluid surrounding the fatty lobules providing a "cobblestone" appearance. (**b**) Shows an extended field of view of the edema and (**d**) demonstrates the edema in 3D. *Abbreviations*: *d* dermis, *st* subcutaneous tissue, *v* vein

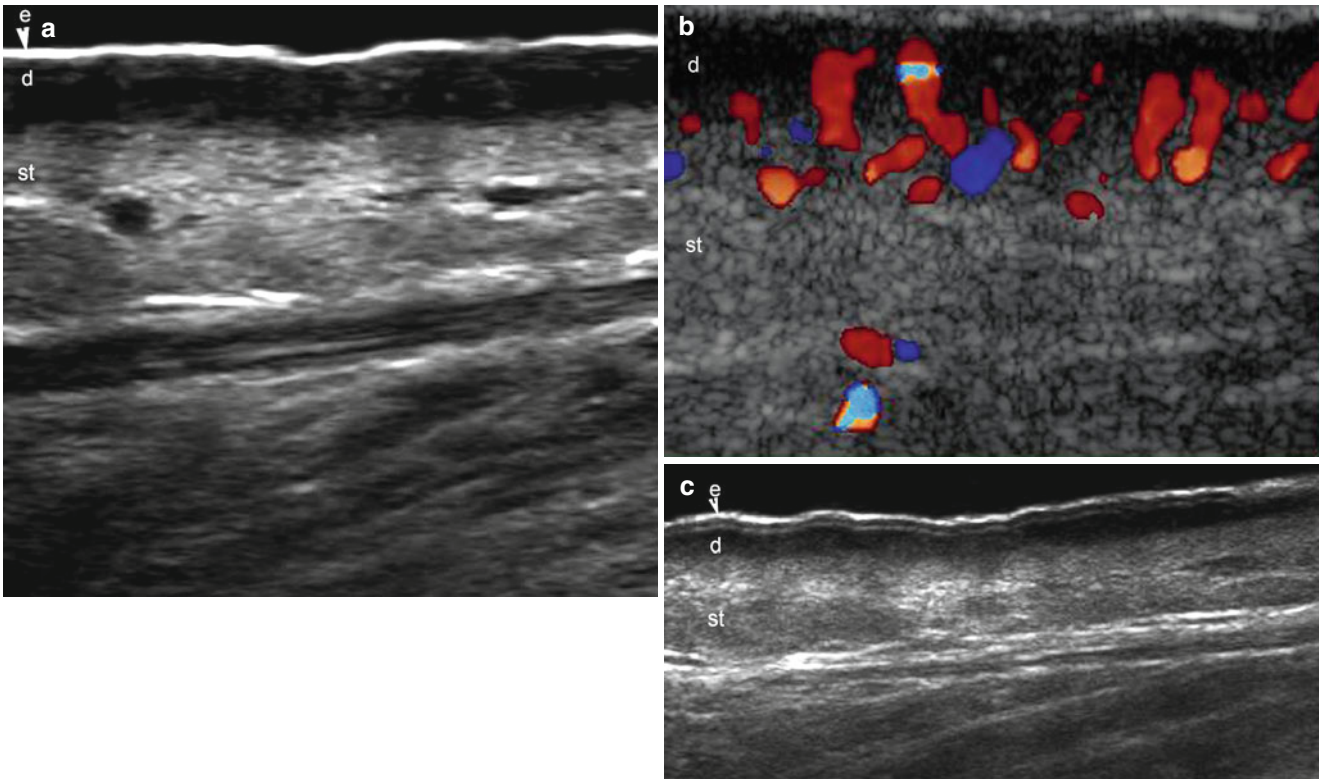

Fig. 4.5 (**a**–**c**) Lymphedema. (**a**) Gray scale ultrasound image shows marked and diffuse hypoechogenicity of the dermis and increased echogenicity of the subcutaneous tissue. Also, notice the prominent hyperechogenicity of the epidermis. (**b**) Color Doppler ultrasound image demonstrates increased vascularity in the dermis. (**c**) Extended field of view (gray scale) shows lymphedema that affect all the cutaneous layers of the leg. Notice the bilaminar appearance of the epidermis that resembles the pattern that is seen in glabrous skin and the prominent decrease of the echogenicity in the dermis and increased echogenicity in the subcutaneous tissue. *Abbreviations*: *e* epidermis, *d* dermis, *st* subcutaneous tissue

4.2.4 Chronic Venous Insufficiency-Lipodermatosclerosis-Liposclerosis

This is the result of an impairment of the main superficial veins and their tributaries that elicit microvascular changes derived from venous ecstasy. Thus, veins and capillaries become dilated, elongated, and tortuous and their endothelium is injured generating an increased extravasation, leading to an enlarged pericapillary space, edema in the interstitial tissue, and to the clinical finding of swelling. Hemoglobin from extravasated erythrocytes in the pericapillary space is degraded to hemosiderin and is responsible for hyperpigmentation. Microthrombosis in the capillaries causes microinfarction and micronecrosis. Hence, skin areas with severe microangiopathy have reduced numbers of perfused nutritional capillaries. Furthermore, the increased blood flow in the deeper skin layers does not contribute to nutrition of the superficial skin layers. The microvascular ischemia is patchy and appears to be the main factor determining trophic changes and venous ulceration. The process of microinfarction and micronecrosis is followed by the formation of a granulation tissue, proliferation of capillaries and fibroblasts, and finally wound healing by formation of scar tissue destroying the microlymphatic network. Clinically this process leads to lipodermatosclerosis, also called liposclerosis (i.e., induration and hyperpigmentation), atrophy, and in its most extreme form, to ulceration where the compensating mechanisms are no longer able to repair the damage. Thus, incompetence of the superficial venous system can generate dilation and secondaryt edema in the skin layers. The most common affected veins are the saphenous venous system (greater and lesser saphenous veins), the perforans veins (i.e., drain superficial structures directly into the deep venous system, therefore, crossing the fascial plane), and communicating veins (i.e., connecting veins in the same fascial plane and venous system). The incompetent vessels and their venous reflux are detectable using sonography, the latter being a feature usually well demonstrated on color Doppler and spectral curve analysis, and mainly when performing the Valsalva maneuver, which is even more evident when the patient is in upright position. Clinically, the skin shows varicose veins (i.e., dilated, tortuous, and palpable veins), reticular veins (i.e., dilated but non-palpable veins), and/or telangiectasias (small reddish to purple non-palpable dilated venous tracts) [12, 13]. Ultrasound has been reported as useful for guiding treatments such as sclerotherapy supporting the localization of the insufficient venous tracts [14]. Lipodermatosclerosis is a consequence of deep venous insufficiency and a risk factor for the occurrence of venous leg ulceration. It is characterized by induration and hyperpigmentation of the skin involving one or both of the lower legs in a characteristic "inverted champagne bottle" appearance. Associated with venous insufficiency, chronic lipodermatosclerosis is most common in middle-aged women. In addition to the chronic form of presentation there is an acute form that exhibits symptoms of severe pain. On sonography, lipodermatosclerosis presents as a diffuse thickening and decreased echogenicity of the dermal layer commonly associated with superficial venous insufficiency signs [15–17] (Figs. 4.6, 4.7 and 4.8).

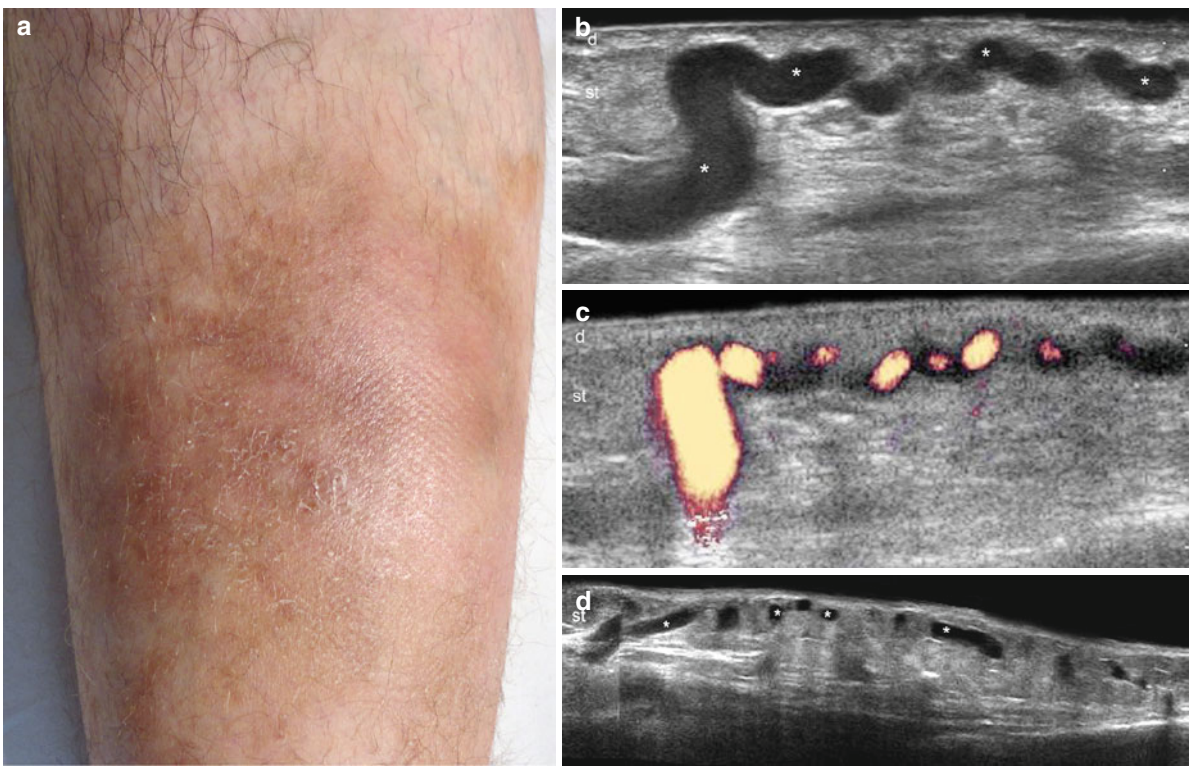

Fig. 4.6 (**a**–**d**) Venous insufficiency. (**a**) Clinical view shows hyperpigmentation and swelling in the anterior aspect of the leg. (**b**) Gray scale ultrasound image (longitudinal view) demonstrates dilated and tortuous perforans venous vessels (*) affecting mostly the upper subcutaneous tissue. (**c**) Power Doppler ultrasound image (longitudinal view) demonstrates flow within the vessels. (**d**) Gray scale ultrasound image (longitudinal extended field of view) shows a wider view of the venous vessels (*) and increased echogenicity of the underlying subcutaneous tissue. *Abbreviations*: *d* dermis, *st* subcutaneous tissue

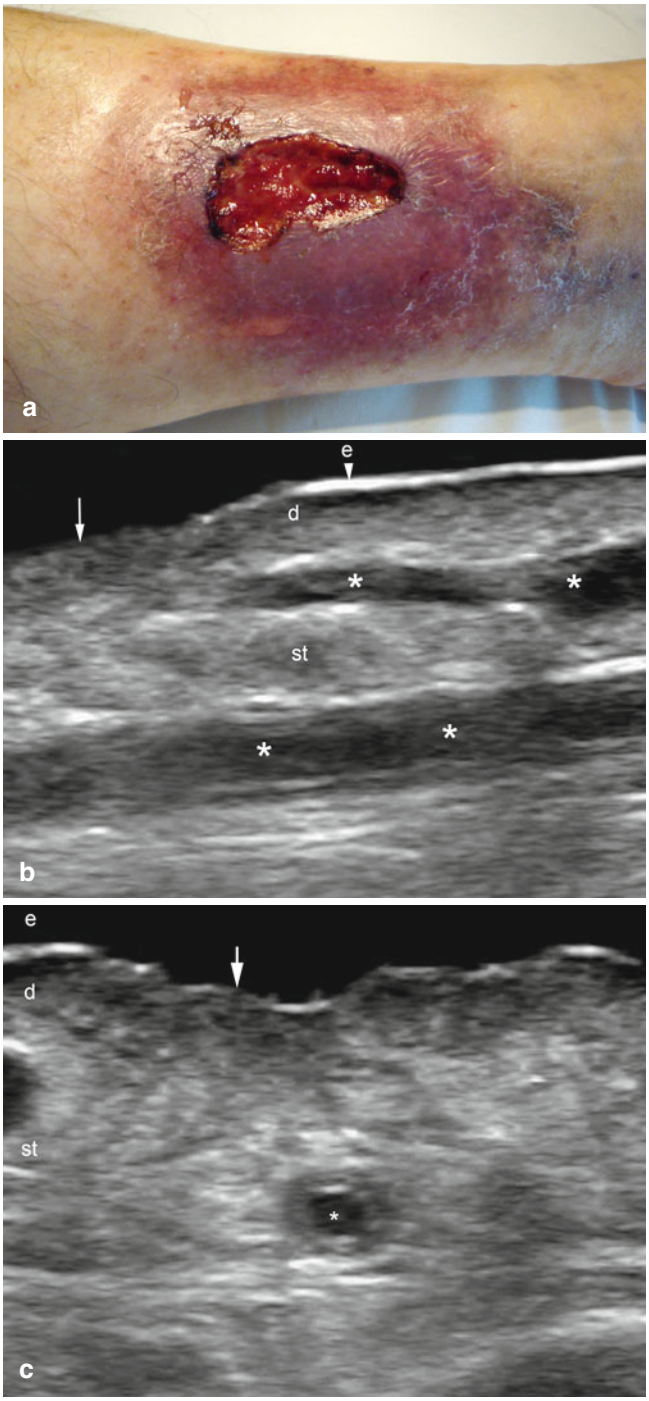

Fig. 4.7 (**a**–**c**) Venous ulcer. (**a**) Clinical lesion. (**b**) Gray scale ultrasound image (longitudinal axis) at the border of the ulcer shows interruption of the epidermis (*arrow*) and dilated anechoic venous vessels (*) in the underlying subcutaneous tissue. Increased echogenicity of the subcutaneous fatty tissue is also detected. (**c**) Gray scale ultrasound image (transverse view) demonstrates increased thickness of the wall of a subcutaneous venous vessel (*) secondary to inflammation. The *arrow* is pointing out the disruption of the epidermal layer. *Abbreviations*: *e* epidermis (*arrowhead*), *d* dermis, *st* subcutaneous tissue

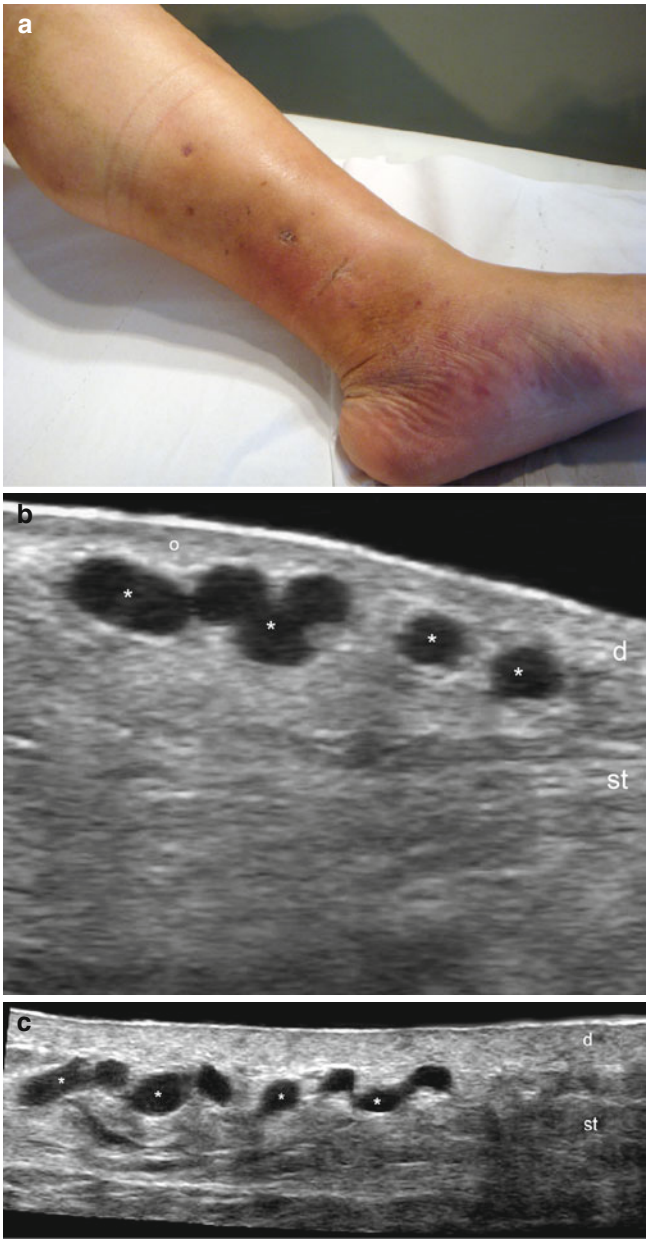

Fig. 4.8 (**a**–**c**) Chronic venous insufficiency. (**a**) Clinical image shows swelling and light pigmentation of the medial aspect of the leg. (**b**) Gray scale ultrasound image (longitudinal view) shows dilated and tortuous anechoic venous vessels (*) in the upper subcutaneous tissue. There is decreased echogenicity of the dermis (*, *d*) and increased echogenicity of the subcutaneous tissue. (**c**) Gray scale ultrasound image (longitudinal extended field of view) demonstrates the wide extension of the dilated and tortuous subcutaneous venous tracts (*). *Abbreviations*: *d* dermis, *st* subcutaneous tissue

4.2.5 Panniculitis

Panniculitis implies the presence of inflammation in the adipose tissue of the subcutaneous layer. It can be associated with a wide range of systemic diseases or local injuries such as trauma or cold, among others.

Clinically, panniculitis is characterized by red, purplish, or skin-colored lumps. Nevertheless, the clinical features frequently show low specificity and can cause trouble with obtaining a diagnosis on the physical examination.

Panniculitis is usually somewhat mixed because the inflammatory infiltrate involves both the septa and lobules; however, histologically, panniculitis can be classified according to the main affected component in the subcutaneous tissue, hence it can be separated into two types: septal and lobular panniculitis, and then each subtype can be subdivided according to presence of vasculitis as follows:

1. Septal panniculitis with vasculitis
2. Septal panniculitis without vasculitis
3. Lobular panniculitis with vasculitis
4. Lobular panniculitis without vasculitis

Septal panniculitis with vasculitis includes leukocytoclastic vasculitis involving the small blood vessels of the septa; superficial thrombophlebitis resulting from inflammation and subsequent thrombosis of large veins of the septa; and cutaneous polyarteritis nodosa, which is a vasculitis that involves the arteries and arterioles of the septa of subcutaneous fat with few or no systemic manifestations. Often septal panniculitis without vasculitis is the consequence of dermal inflammatory processes extending to the subcutaneous fat, such as necrobiosis lipoidica, subcutaneous granuloma annulare, scleroderma, rheumatoid nodule, and necrobiotic xanthogranuloma. However, in other cases, the inflammatory process is primarily located in the fibrous septa of the subcutis with or without involvement of the overlying dermis such as in erythema nodosum, the most frequently seen septal panniculitis (without vasculitis). Erythema nodosum in fully developed lesions is characterized histopathologically by Miescher's radial granulomas in the septa. On sonography, septal panniculitis (SP) shows prominent thickening and hypoechogenicity of the septa, in addition to the increased echogenicity of the fatty tissue. In contrast, lobular panniculitis primarily affects the lobules of the fatty subcutaneous tissue and can be observed in a wide spectrum of diseases such as erythema induratum of Bazin (nodular vasculitis), the most common variant of lobular panniculitis with vasculitis, or sclerosing panniculitis that results from chronic venous insufficiency of the lower extremities; calciphylaxis and oxalosis, which implies panniculitis with calcification of the vessel walls, sclerema neonatorum, an inflammatory disease with crystals within the adipocytes, subcutaneous fat necrosis of the newborn, and post-steroid panniculitis, among others. Lobular panniculitis may also be an expression of infections, trauma, or factitial causes involving subcutaneous fat. Lipodystrophies are common sequelae of panniculitis and can be separated in hypertrophic or atrophic, according to the increase or decrease in the fatty component [18–20]. On sonography, lobular panniculitis presents as marked blurriness and increased echogenicity of the fatty lobules of the subcutaneous tissue. Although the septa may present some degree of thickening and hypoechogenicity, these changes are less prominent compared with SP. In the presence of fat necrosis, anechoic or hypoechoic round-shaped pseudocystic structures have been reported as the result of fat liquefaction [21]. On color Doppler imaging, vascularity can be variable going from low to high although the hypovascularity in the subcutaneous tissue on the ultrasound examination does not detract the presence of vasculitis. Therefore, the primary role of ultrasound should be directed to assess the presence of panniculitis and ideally support the difference between mostly septal or lobular panniculitis (Figs. 4.9, 4.10, 4.11, 4.12 and 4.13).

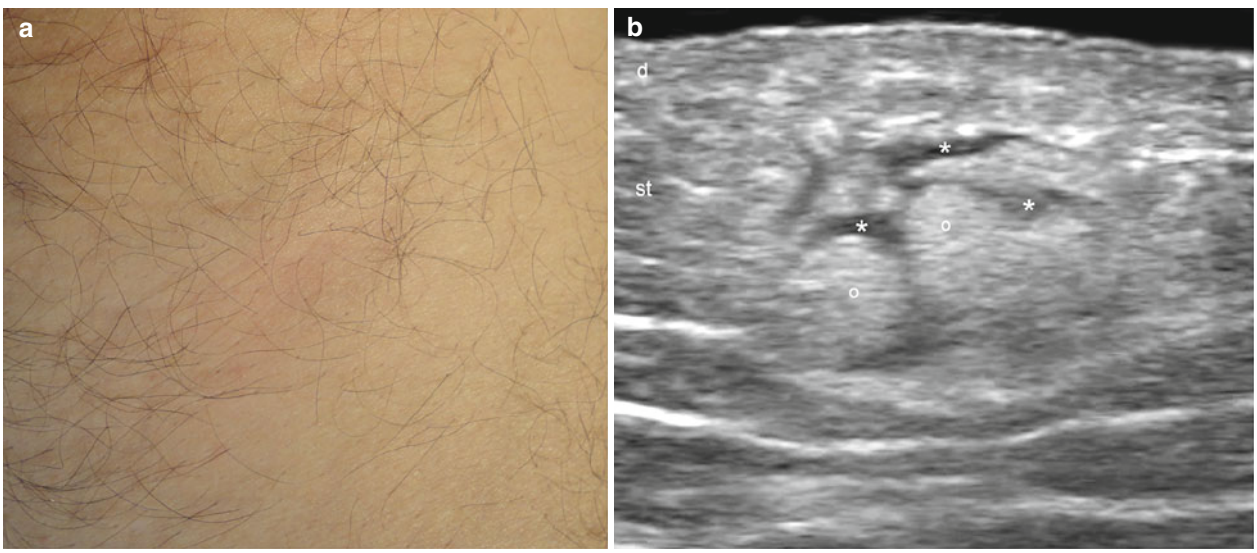

Fig. 4.9 (**a**–**e**) Mostly septal panniculitis. (**a**) Clinical image shows slight erythema and induration. (**b**) Gray scale (longitudinal view) demonstrates focal increased echogenicity of the fatty lobules (o) of the subcutaneous tissue with prominent hypoechoic septa (*). (**c**) Color Doppler ultrasound image (longitudinal view) shows a thick vessel running through the lesional area. (**d**) The lesional area in 3D (5–8 s transverse axis sweep). (**e**) Histology (HE 100× zoom) shows thickening and inflammation of the septa (*arrows*) that surround the fatty lobules (o) of the subcutaneous tissue. *Abbreviations*: *e* epidermis, *d* dermis, *st* subcutaneous tissue

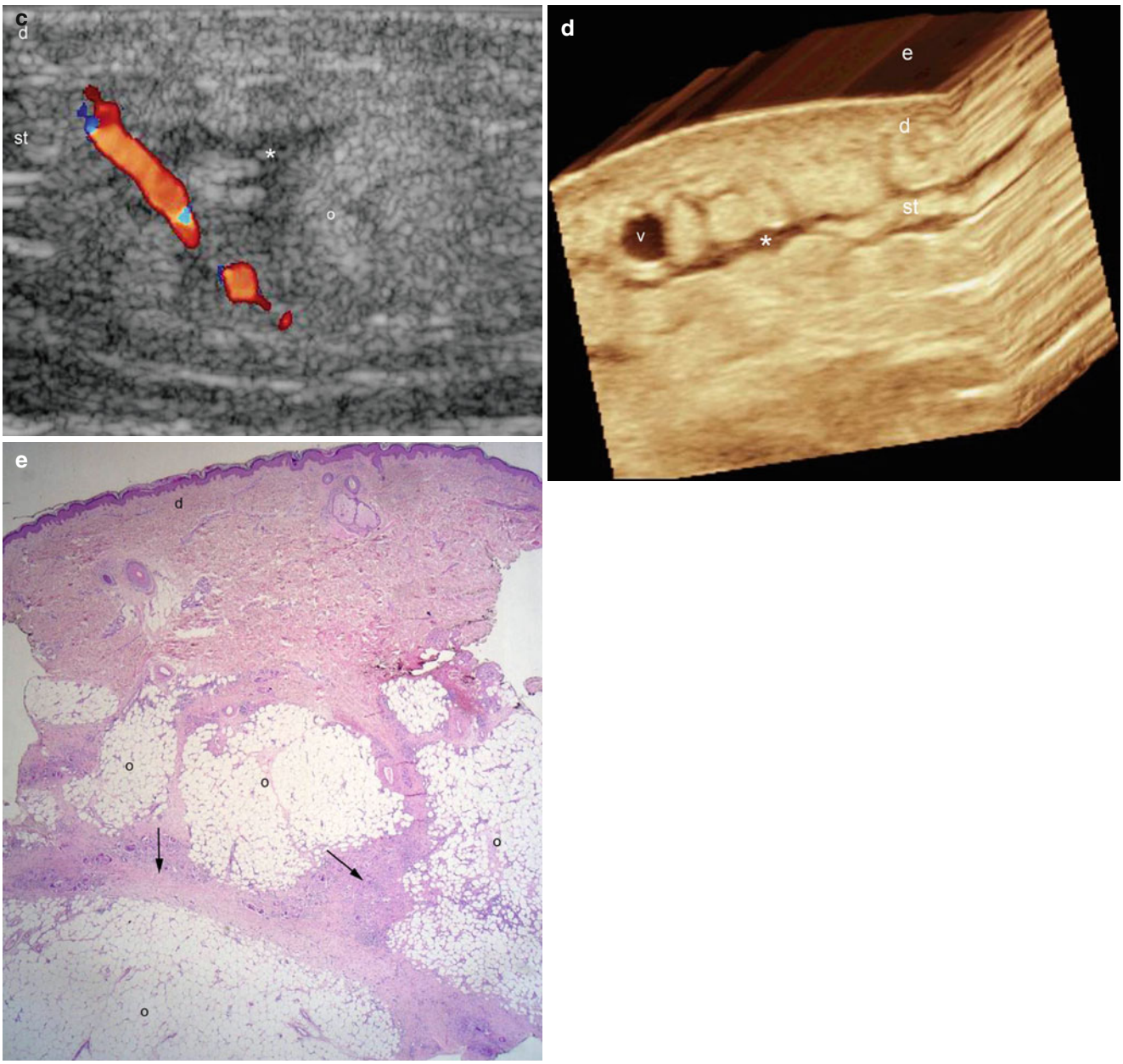

Fig. 4.9 (continued)

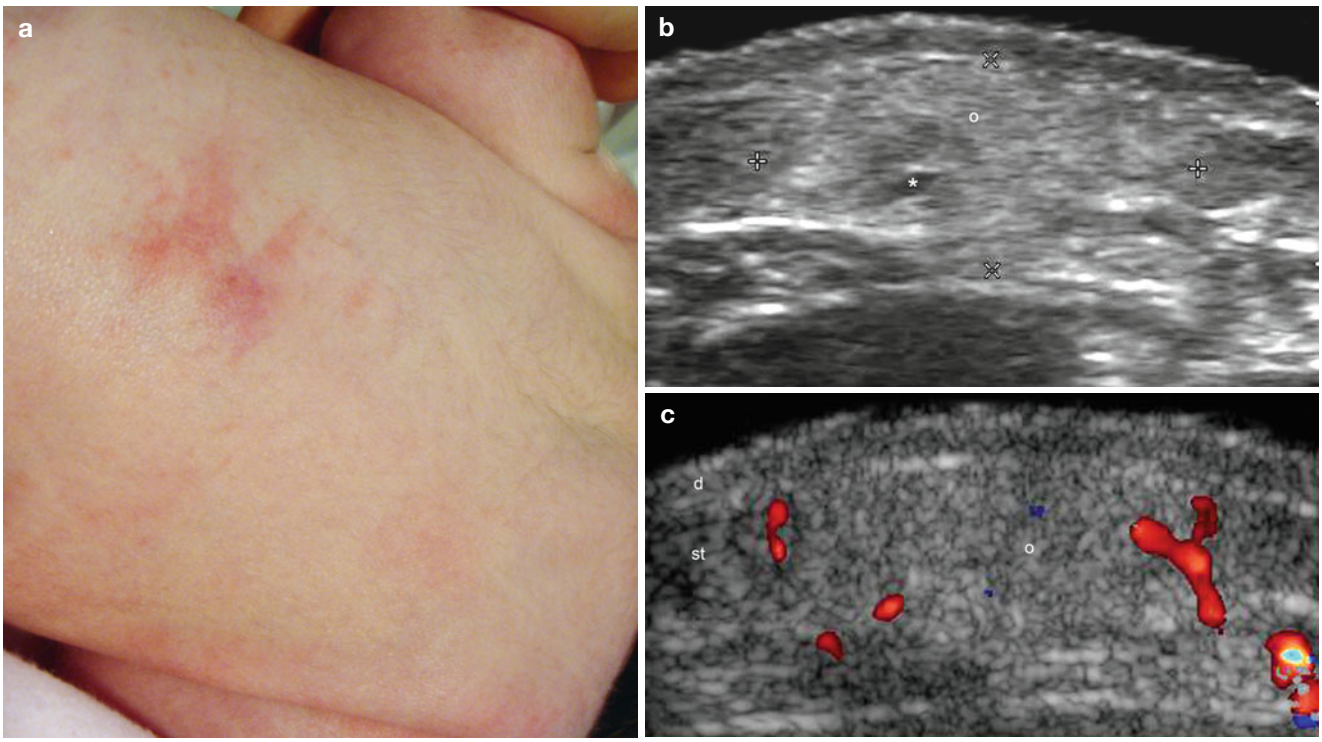

Fig. 4.10 (**a**–**c**) Mostly lobular panniculitis. Fat Necrosis of the newborn. (**a**) Clinical image shows erythema and swelling in the dorsolumbar region in a newborn. (**b**) Gray scale ultrasound image (transverse view) demonstrates increased echogenicity of the fatty lobules of the subcutaneous tissue with blurriness of the borders of the lobules (o). In-between the fatty tissue there is a small anechoic round-shape pseudocystic hypoechoic structure (*) that corresponds to a fat liquefaction area. (**c**) Color Doppler ultrasound image (transverse view) shows increased vascularity in the periphery of the lesional area and hypovascularity within the lesion (o). *Abbreviations*: *d* dermis, *st* subcutaneous tissue

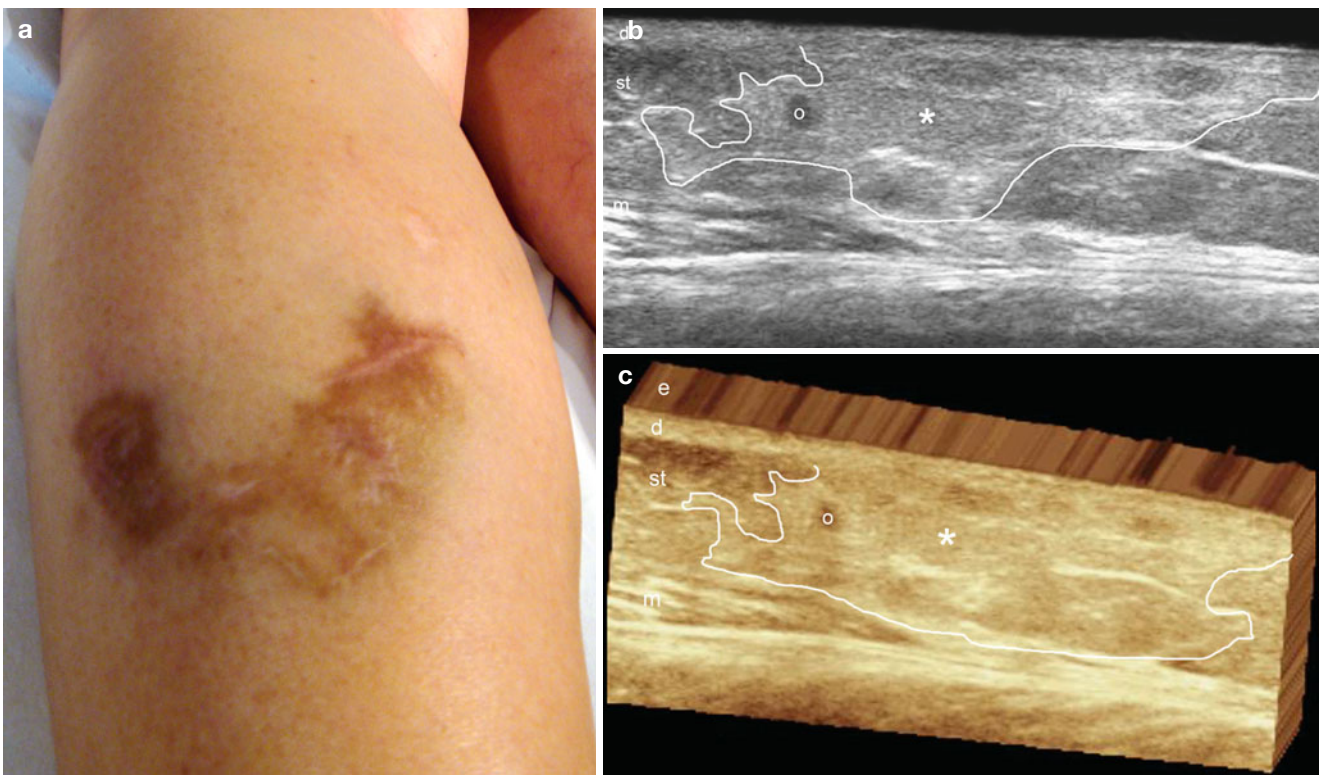

Fig. 4.11 (**a**–**c**) Mostly lobular panniculitis secondary to a dog bite. (**a**) Clinical lesion 8 months after dog bite in the calf shows a scarring, swelling and hyperpigmentation. (**b**) Gray scale ultrasound image (longitudinal view) demonstrates increased echogenicity and blurriness of the fatty lobules of the subcutaneous tissue (* and outlined) and a focal pseudocystic round-shaped hypoechoic structure (o) that corresponds to a liquefaction area of the fat (fat necrosis). (**c**) The lesion in 3D (5–8 s sweep). *Abbreviations*: *e* epidermis, *d* dermis, *st* subcutaneous tissue, *m* medial gastrocnemious muscle

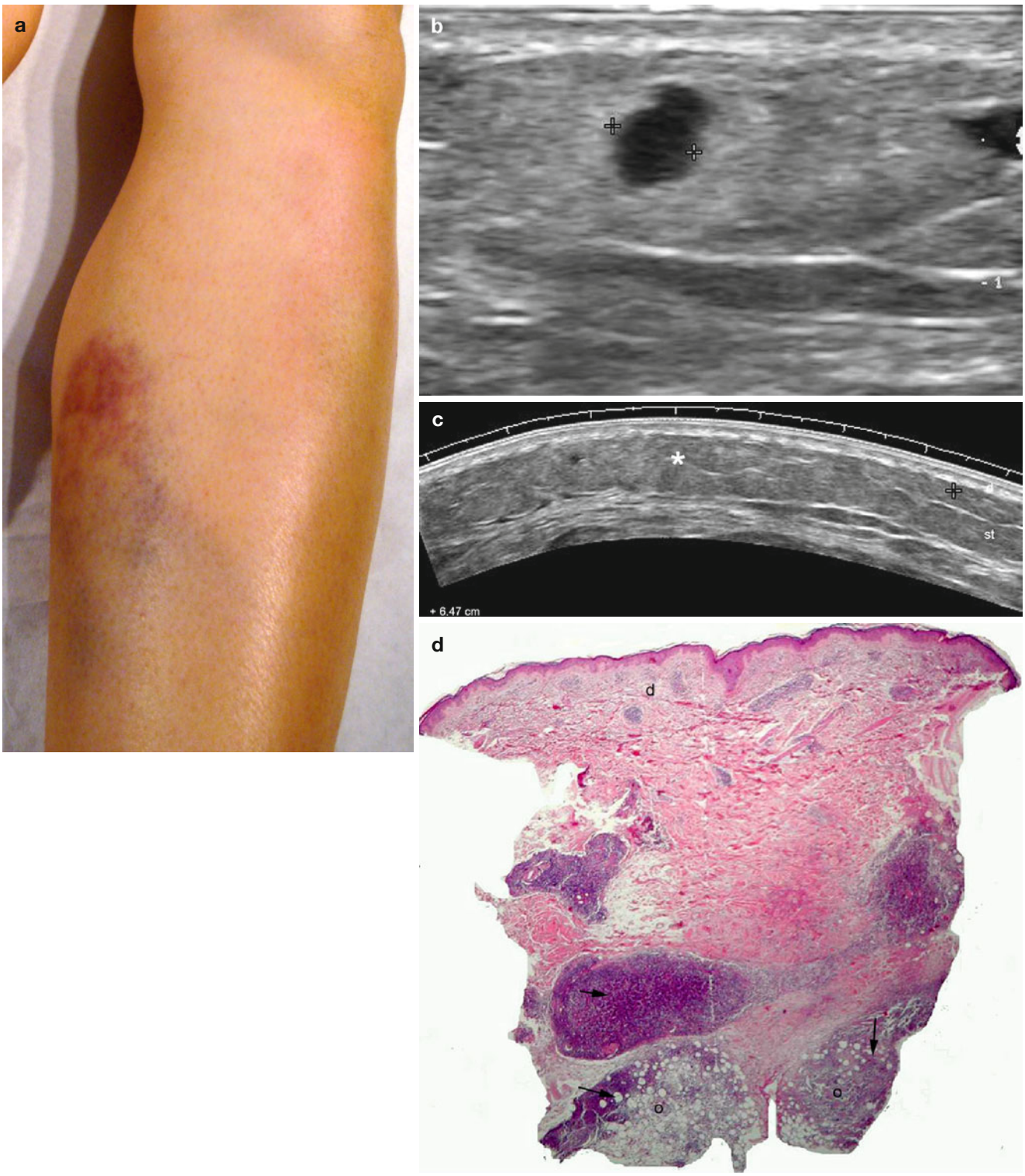

Fig. 4.12 (**a**–**d**) Mostly lobular panniculitis secondary to insect bite. (**a**) Clinical lesion shows erythema and ecchymosis in the site of the bite (spider). (**b**) Gray scale ultrasound image (longitudinal view) demonstrates increased echogenicity of the subcutaneous tissue and a round-shaped anechoic pseudocystic structure (between markers) that corresponds to fat liquefaction (fat necrosis). (**c**) Gray scale ultrasound image (transverse extended field of view) demonstrates a 6.47 cm area with increased echogenicity of the subcutaneous tissue. Notice the blurriness of the borders of the lobules and the septa in the lesional area. (**d**) Histology (HE 20× zoom) shows inflammatory infiltrates (*arrows*) affecting the fatty lobules (o) of the subcutaneous tissue. *Abbreviations*: *d* dermis

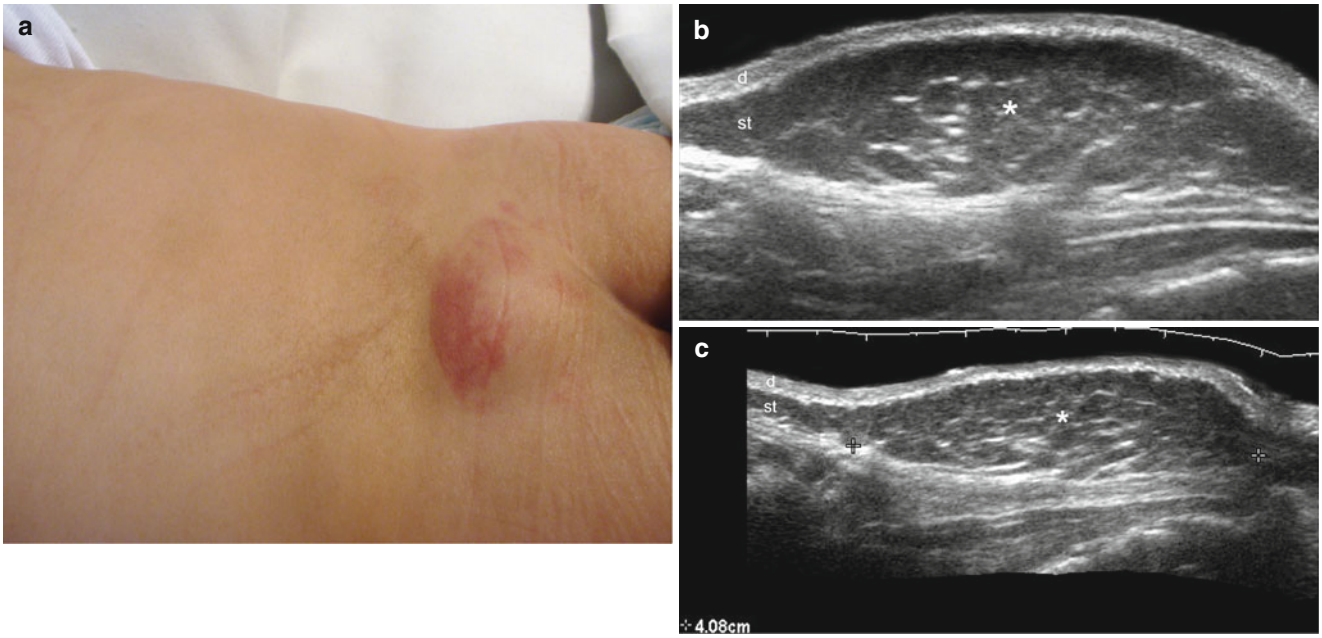

Fig. 4.13 (**a**–**c**) Hypertrophic lipodystrophy (congenital). (**a**) Clinical lesion in the lumbosacral region shows swelling and erythema. (**b**) Gray scale ultrasound image (transverse view) demonstrates a focal region with increased thickness of the subcutaneous tissue. No well-defined nodular structure or capsule can be detected. (**c**) Gray scale ultrasound image (longitudinal view) shows a 4.08 cm long lesional tissue (*, between markers) with increased thickness of the subcutaneous tissue. Notice that there is no abnormality in the echostructure of the subcutaneous tissue or the dermal layer. *Abbreviations*: *d* dermis, *st* subcutaneous tissue

4.2.6 Odontogenic Fistula

These fistulous tracts are commonly originated in dental inflammatory and infectious processes that drain into the soft tissues and open into the subepidermal or epidermal zones, commonly the maxillae or mandibular regions of the face. Clinically, these odontogenic fistulae may mimic a dermatologic origin, appearing as erythematous or bluish papulae that could drain viscous fluid. These lesions can also clinically mimic malignant skin tumors.

On sonography, the fistulous tracts usually appear as hypoechoic, sometimes slightly heterogeneous bands. The connection between the bony margin of the maxillae or mandible is usually assessed using sonography and commonly an erosion can be detected in the bony margin. With color Doppler imaging there is frequently hypervascularity in the periphery of the tracts [22, 23] (Figs. 4.14 and 4.15).

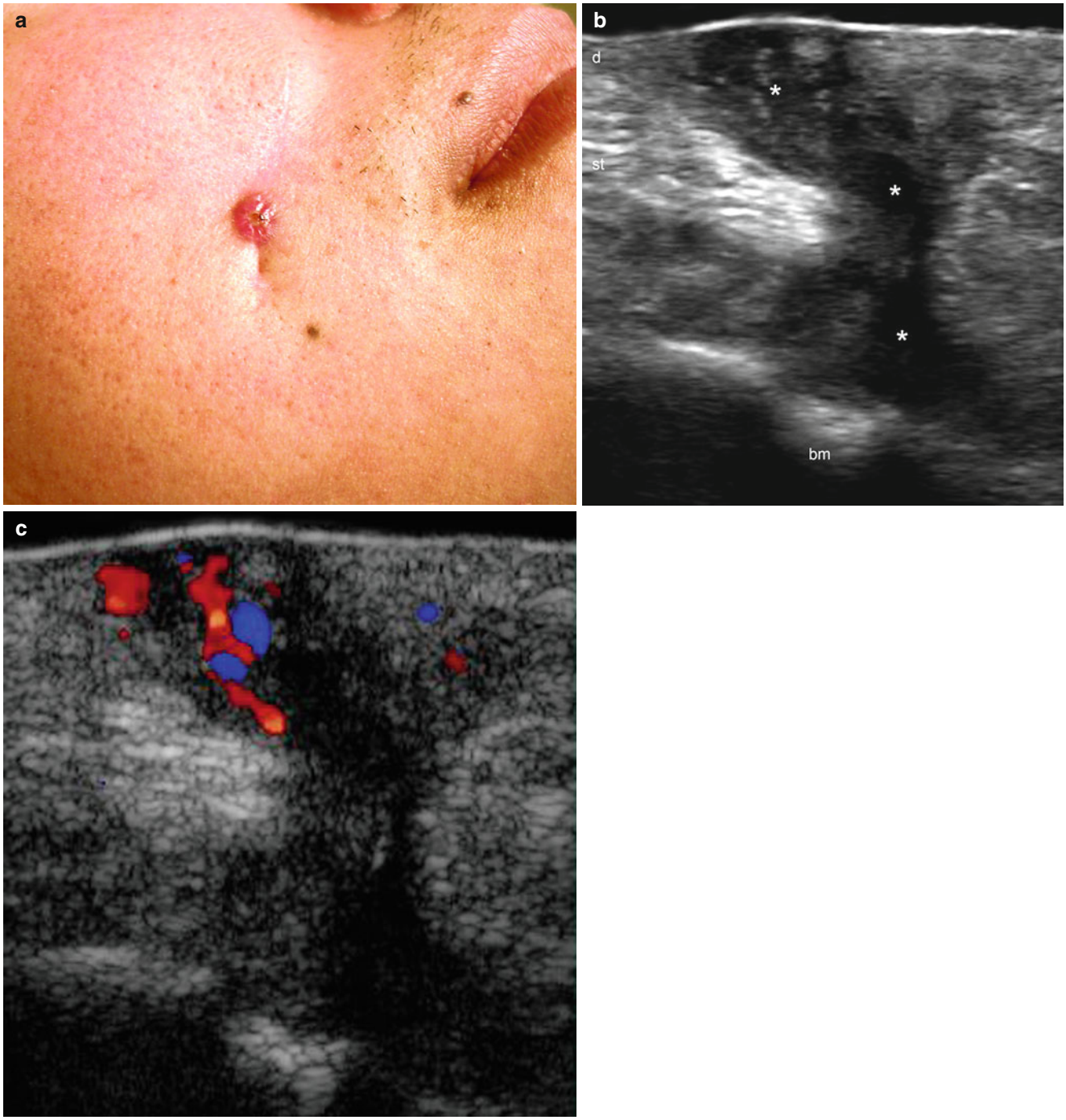

Fig. 4.14 (**a**–**c**) Odontogenic fistula. (**a**) Clinical lesion shows erythematous papule in the right cheek. (**b**) Gray scale ultrasound image (oblique longitudinal view) demonstrates tortuous hypoechoic fistulous tract (*) that connects the dermis and subcutaneous tissue with the bony margin of the upper maxilla. Notice the scalloping of the bony margin (*bm*) at the site of attachment of the fistula. (**c**) Color Doppler ultrasound image (oblique longitudinal view) shows increased vascularity in the periphery of the fistula. *Abbreviations*: *d* dermis, *st* subcutaneous tissue

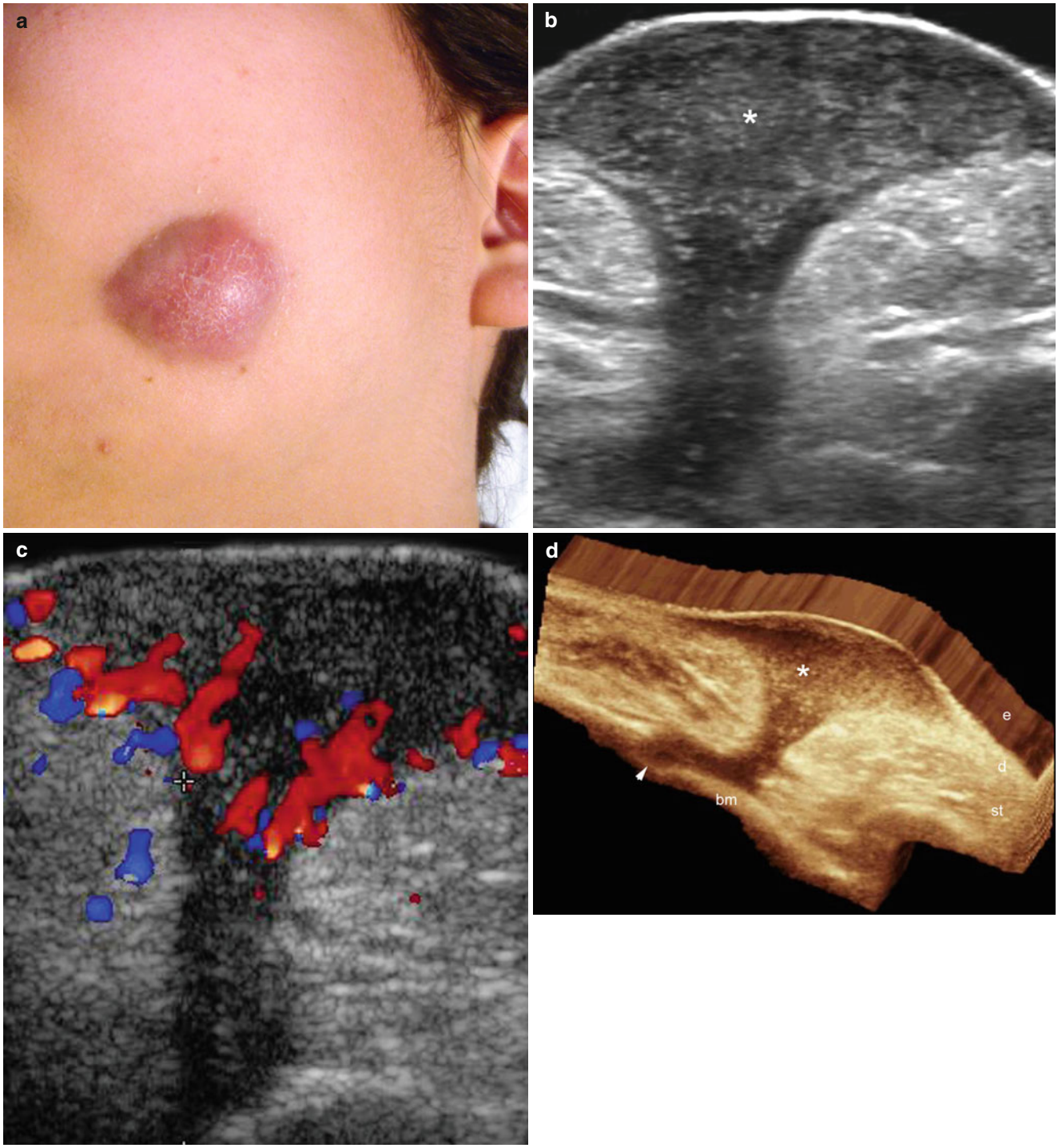

Fig. 4.15 (**a**–**d**) Odontogenic fistula. (**a**) Clinical lesion shows erythematous nodule in the left cheek. (**b**) Gray scale ultrasound image (transverse view) demonstrates hypoechoic "champignon-shaped" structure (*) in the dermis and subcutaneous tissue wider in the surface and narrow in the deepest portion (hypoechoic tract). (**c**) Color Doppler ultrasound image (longitudinal view) shows increased vascularity in the periphery of the lesional area. (**d**) 3D reconstruction of the fistula clearly shows the attachment of the fistula to the bony margin of the upper maxilla (scalloping area of the bone that is pointed out with an *arrow*). *Abbreviations*: *e* epidermis, *d* dermis, *st* subcutaneous tissue, *bm* bony margin of the upper maxilla

4.2.7 Mondor's Disease

Mondor's disease is a superficial vein thrombosis usually located in the subcutaneous tissue. The clinical sign is a cord-like palpable structure that tends to disappear over time. On sonography, the affected venous tract can be recognized as a tubular hypoechoic structure in correlation with the cord-like structure. Occasionally increased echogenicity of the subcutaneous tissue that surrounds the superficial vein can be found. On color Doppler imaging, no flow is detectable within the vessel in the acute phase. After a few weeks, the vascularity may return in concordance with the disappearance of the palpable cord-like structure and the ultrasound changes. Importantly, sonography may provide a tool to differentiate Mondor's disease from linear morphea [24] (Fig. 4.16).

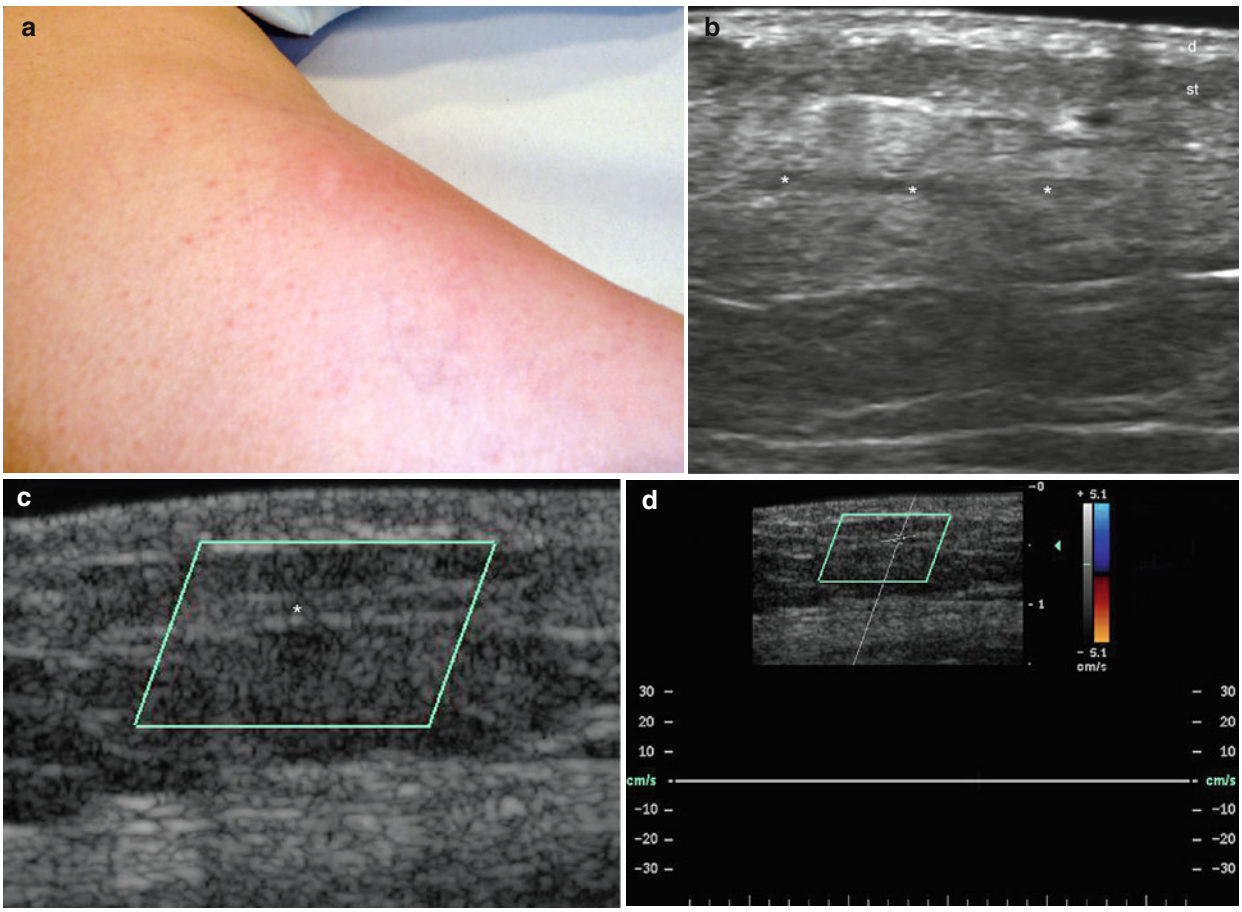

Fig. 4.16 (**a**–**d**) Mondor's disease. (**a**) Clinical image shows erythema in the medial aspect of the right thigh. There was also a palpable cord-like structure. (**b**) Gray scale ultrasound image (longitudinal view) demonstrates a dilated vessel in the subcutaneous tissue filled with hypoechoic thrombotic material (*). Increased echogenicity is detected in the surrounding subcutaneous tissue. (**c**) Color Doppler ultrasound image (longitudinal view) shows no vascularity within the vessel (*). (**d**) Color Doppler spectral curve analysis confirms the lack of vascularity. *Abbreviations*: *d* dermis, *st* subcutaneous tissue

4.2.8 Warts

Warts are common entities caused by the infection with the human papilloma (HP) virus and can generate painful lesions that can clinically mimic a foreign body or Mortons' neuroma when they are located in the plantar region. On physical examination, warts present as painful hyperkeratotic lesions frequently located in the soles of the feet. Warts can also affect other regions of the body, such as the hands. The HP virus causes an ingrown proliferation that usually shows an oval fusiform hypoechoic structure on sonography that affects the epidermis and dermis. Vascularity is variable and can go from hypo- to hypervascular in the sublesional dermis. Additionally, inflammatory changes in the vicinity of the wart that commonly affect the underlying plantar bursae can be detected. Painful warts (symptomatic) are usually associated with a higher presence of vascularity and bursitis [25, 26] (Figs. 4.17, 4.18, 4.19, 4.20 and 4.21).

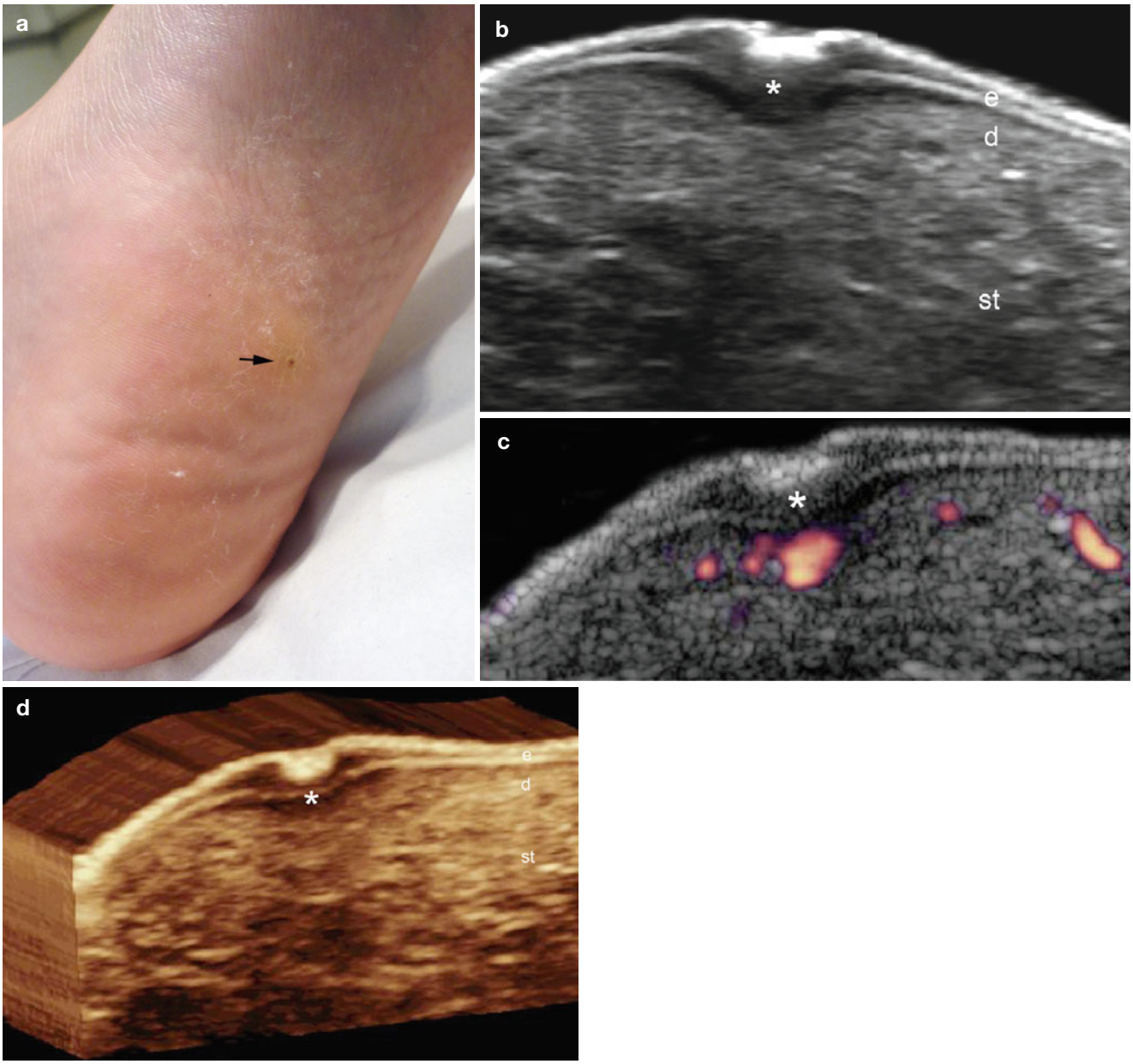

Fig. 4.17 (**a**–**d**) Plantar wart. (**a**) Clinical image shows hyperkeratotic lesion in the sole of the left foot. (**b**) Gray scale ultrasound image (transverse view) demonstrates fusiform shaped hypoechoic structure (*) that involves epidermis and dermis. The central hyperechoic epidermal depression corresponds to the clinical scab. (**c**) Color Doppler power angio (transverse view) demonstrates increased sublesional blood flow. (**d**) The lesion (*) in 3D (5–8 s reconstruction). *Abbreviations*: *e* epidermis, *d* dermis, *st* subcutaneous tissue

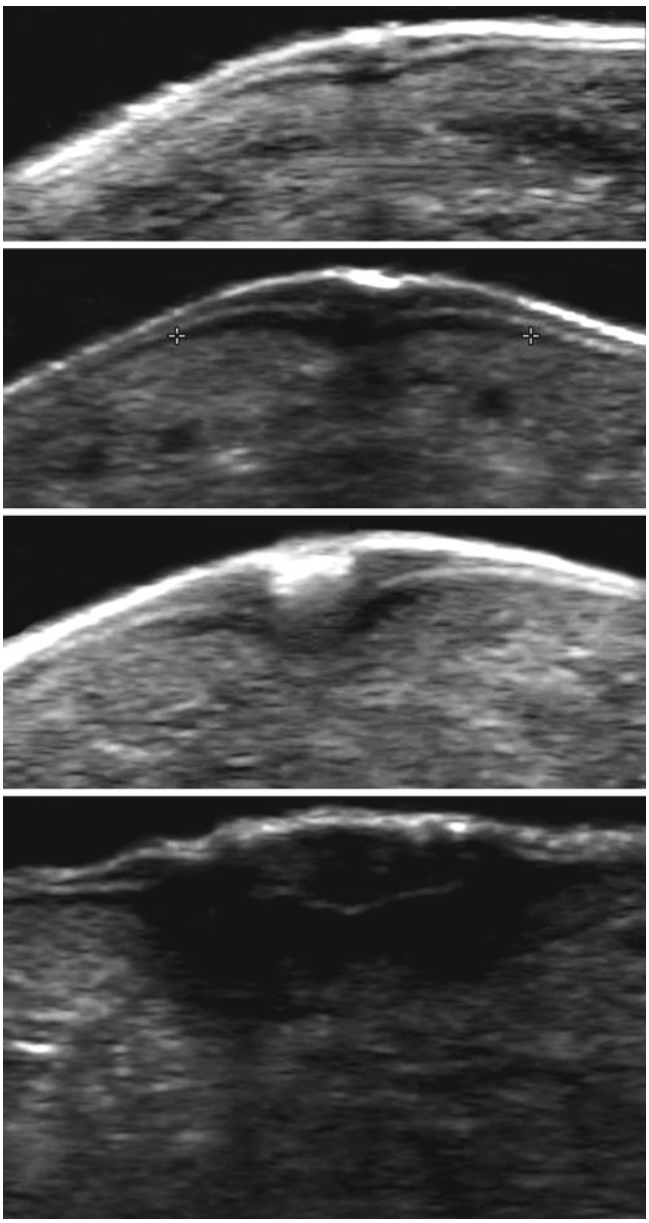

Fig. 4.18 Degree of depth involvement in plantar warts going from superficial (*top*) to deep (*bottom*). Notice the ingrown pattern of involvement of the warts within the cutaneous layers

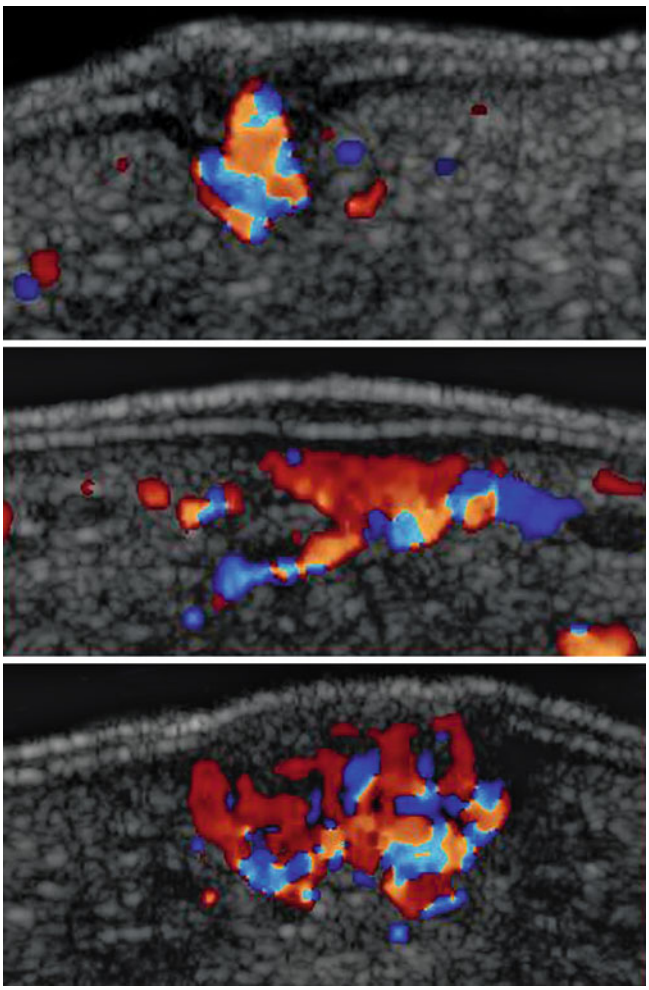

Fig. 4.19 Degree of vascularization of plantar warts going from hypovascular (*top*) to hypervascular (*bottom*)

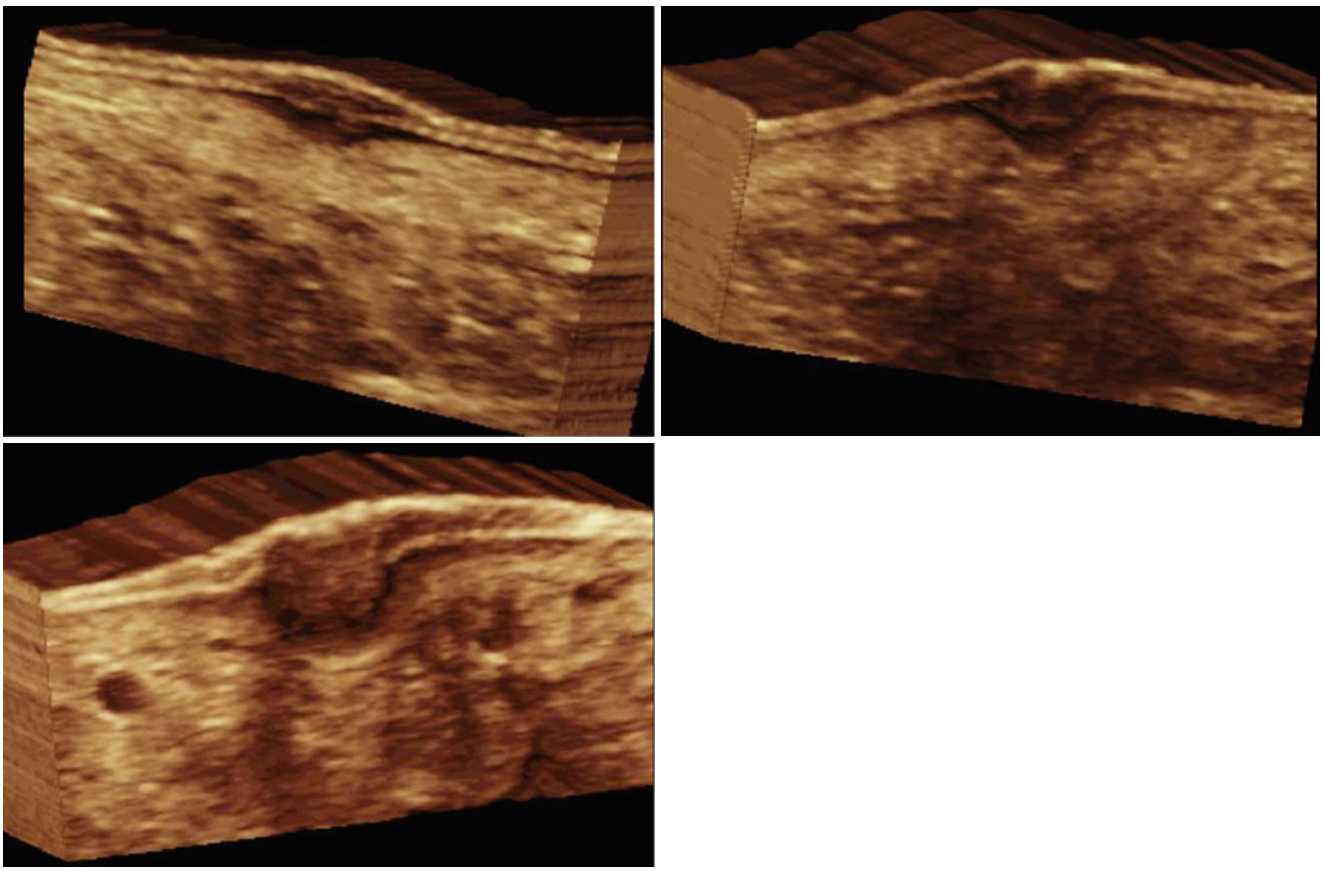

Fig. 4.20 3D reconstructions (5–8 s sweep) of the patterns of involvement in plantar warts

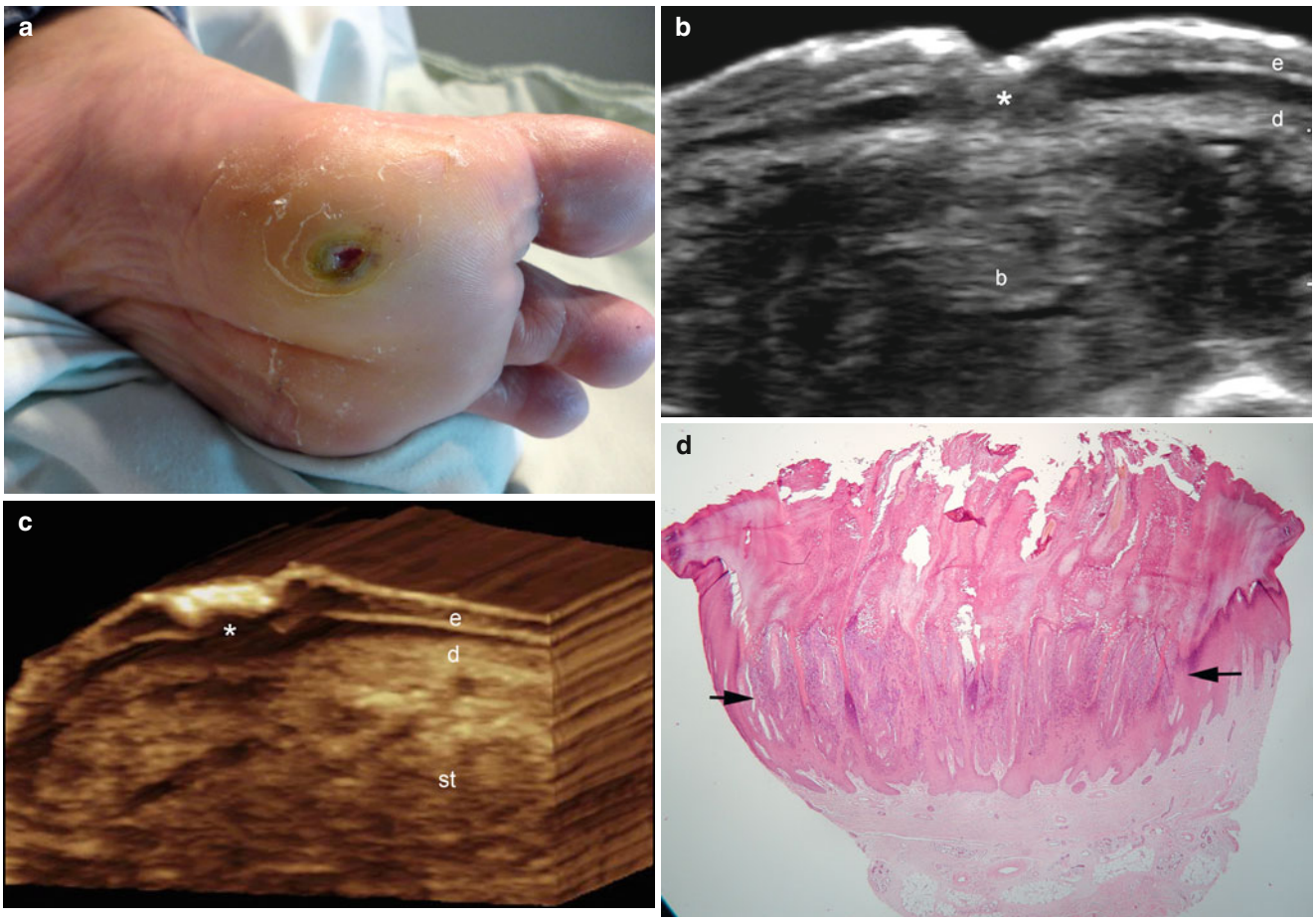

Fig. 4.21 (**a**–**d**) Plantar wart and bursitis. (**a**) Clinical lesion with ulceration and hyperkeratosis. (**b**) Gray scale ultrasound image (transverse view) shows fusiform shaped hypoechoic involvement (*) of the epidermis and dermis. There is distention and synovial proliferation of the plantar bursa (*b*) underlying the lesion. (**c**) 3D reconstruction of the lesional area (*, 5– 8 s sweep). (**d**) Histology (HE 20× zoom) demonstrates the viral infiltration (*between arrows*) with hyperkeratosis, acanthosis, hypergranulosis and papillomatosis. There is also dilation of venous vessels in the dermal papillae. *Abbreviations*: *e* epidermis, *d* dermis, *st* subcutaneous tissue

4.2.9 Psoriasis

Psoriasis is an autoimmune inflammatory disease that affects the skin, nails, enthesis and joints. Clinically, typical psoriatic plaques are characterized by erythematous, itchy, and elevated areas with increased scaling. Commonly, patients may recognize that new lesions appear at sites of injury to the skin (Koebner's phenomenon). These plaques commonly affect the extensor aspects and the scalp, but there are other forms of presentation that can also involve the flexor and intertriginous areas (i.e., axilla, groin, umbilical region, inframammary folds) with low or absent scaling. Less frequent types of psoriasis are guttate psoriasis, an acute form most commonly found in children after an upper respiratory infection and characterized by small droplike, salmon or pink papules, with fine scales; and pustular psoriasis (localized or generalized) that shows persistent pinhead-sized, sterile, sub-corneal pustules, persistent pustular eruptions of the hands and feet (localized) or affecting the skin in general. These pustules grow and merge into larger regions that can facilitate a secondary bacterial infection. The latter conditions can also affect the oral mucosa and the lips. Erythrodermic psoriasis, another rare and severe form of psoriasis, shows a widespread inflammation and erythroderma (i.e., exfoliative dermatitis) over most of the body surface. It can be accompanied by severe itching, swelling, and pain [27].

Nail involvement is extremely common in psoriasis and affects approximately 50 % of patients. In less than 5 % of the cases, the involvement of the nails can appear without cutaneous lesions. About 10–20 % of people with psoriasis also have psoriatic arthritis, and 80 % of patients with psoriatic arthritis (PsA) present nail psoriasis. Clinical manifestations of nail psoriasis are pitting, discoloration, onycholysis (i.e., separation of the nail plate from the nail bed), and subungual hyperkeratosis as well as nail plate crumbling and splinter hemorrhages [28].

Other types of inflammatory involvement in psoriasis include the joints, enthesis, and the bowel. PsA is a chronic inflammatory arthropathy associated with psoriasis, and is included among the seronegative spondyloarthropathies. The presence of cutaneous psoriasis is very important for correct and early diagnosis of PsA because the cutaneous lesions commonly precede the appearance of joint manifestations [29].

Histologically, psoriatic plaques show acanthosis (elongation of the rete ridges and corresponding dermal papillae), parakeratosis (presence of nucleated inmature keratinocytes in the stratum corneum), orthokeratosis (hypertrophy of the stratum corneum), loss of the granular cell layer, spongiform pustules, dermal mononuclear infiltrates, and parakeratotic microabscesses. At the nail, there is hyperkeratosis of the nail plates. Synovial proliferation is detected in the articular areas [30].

On sonography, psoriatic plaques show thickening of the epidermis and hypoechogenicity and thickening of the upper dermis. Occasionally, undulation of the epidermis can be detected. On color Doppler imaging, increased dermal blood flow is usually detected within the lesions. Ungual sonographic involvement varies according to the phase of activity of the disease, hence, going from early to late phases: thickening and decreased echogenicity of the ungual bed, focal hyperechoic spots in the ventral plates, and wavy plates and thickening of both plates (dorsal and ventral) can be found. Blood flow is usually increased in the proximal nail bed with low flow arterial vessels especially during the active phases of the disease. Joints can show prominent synovium, anechoic fluid, and periarticular erosions commonly in the interphalangeal joints. Tendinopathy that shows hypo- or heterogeneous echogenicity, usually at the insertion sites of the tendineous structures, has also been sonographically reported in patients with psoriasis even at subclinical stages. Increased blood flow may detected in the synovium on color Doppler imaging in active phases. Sonographic monitoring of treatment in psoriasis has been recently reported [31–33] (Fig. 4.22).

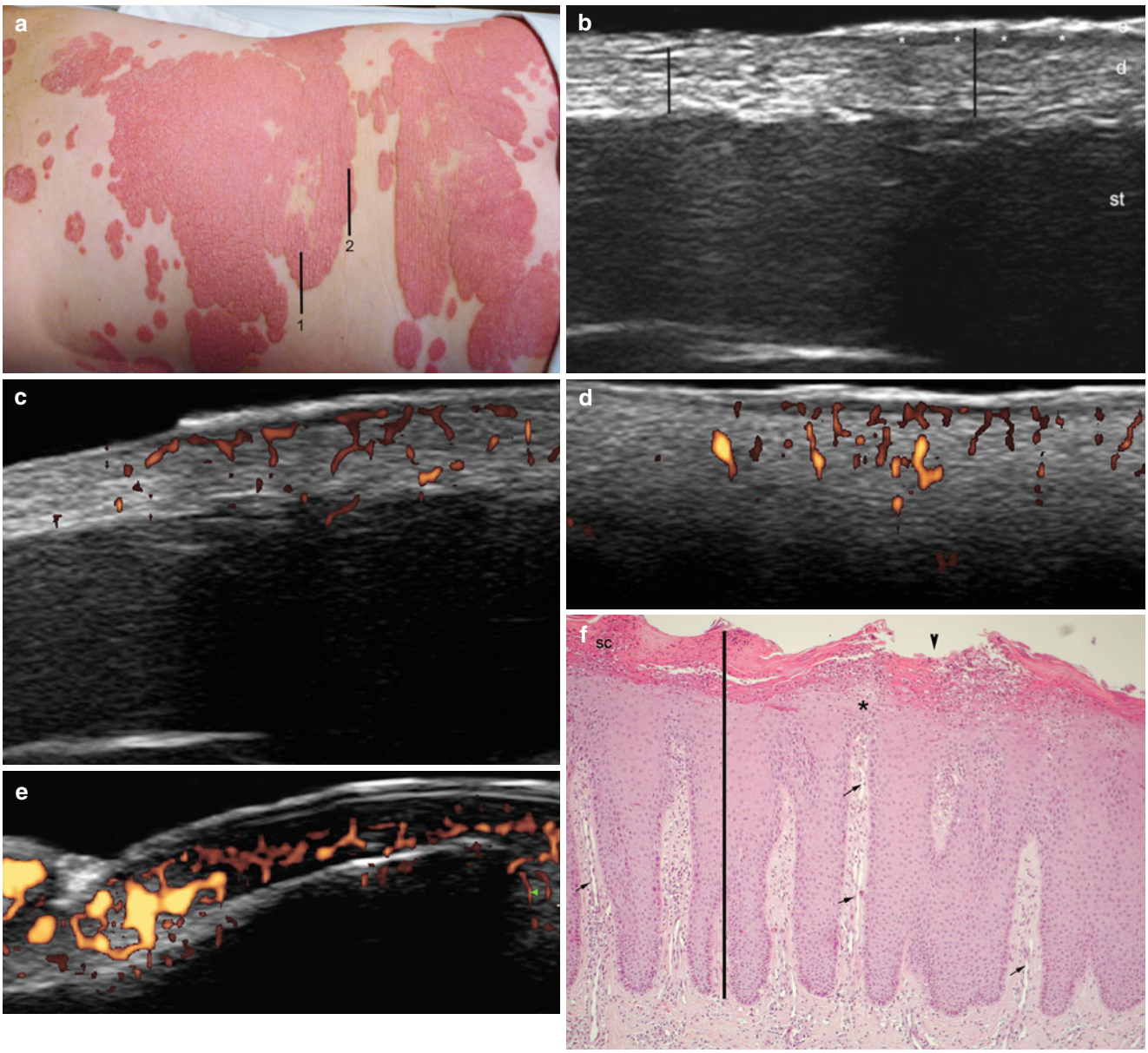

Fig. 4.22 (**a**–**f**). Psoriasis. (**a**) Clinical image shows multiple erythematous psoriatic plaques in the dorsolumbar region. The *black lines* [1, 2] show the orientation of the following ultrasound images. (**b**) Gray scale ultrasound image (transverse view, line 1 in (a)) demonstrates thickening of the epidermis and dermis with an hypoechoic band (*) in the upper dermis. The *vertical black lines* illustrate the different thicknesses in the abnormal (plaque, right side) and normal skin (*left side*). (**c**) Power Doppler ultrasound image (transverse view, line 1 in (a)) demonstrates increased blood flow in the upper dermis of the psoriatic plaque. (**d**) Power Doppler ultrasound image (transverse view, line 2 in (a)) shows similar morphology of the hypervascularity in the psoriatic plaque (*right side*) in comparison with the normal skin (*left side*) (**e**) Power Doppler ultrasound image of the nail (longitudinal view) of the left thumb in the same patient shows increased vascularity in the ungual bed. (**f**) Histology (HE 100 × zoom) demonstrates hyperkeratosis, acanthosis, agranulosis and suprapapillary thinning (*) of the epidermis (*black line*). There is also a small pustule in the stratum corneum (*arrowhead*) and prominent vascularity (*arrows*). *Abbreviations*: *e* epidermis, *d* dermis, *st* subcutaneous tissue, *sc* stratum corneum

4.2.10 Morphea

Also known as localized scleroderma, morphea is a fibrosing disorder of the skin and underlying tissues. Morphea is differentiated from systemic sclerosis because of the absence of sclerodactyly, Raynaud phenomenon, and nail fold capillary changes. Nevertheless, patients with morphea commonly have systemic symptoms such as malaise, fatigue, arthralgias, and myalgias, as well as positive autoantibody serologies. However, morphea is almost uniformly limited to those tissues derived from the mesoderm. The underlying pathogenesis of morphea is not completely understood at this time, but ultimately it results in an imbalance of collagen production and destruction. Early morphea lesions present as erythematous to purple indurated lesions that turn into sclerotic, atrophic, hairless plaques with varying amounts of post-inflammatory hyperpigmentation. There are several clinical subtypes of morphea, the most common is the plaque type, also called circumscribed morphea, that presents as fewer that three discrete indurated plaques. The superficial variant is more frequent and localized and limited to the epidermis and dermis. The deep variant of plaque morphea is also called subcutaneous or deep; morphea can affect the subcutaneous tissue, fascia, and muscular layers. Some classifications included in the plaque-morphea variants are the guttate (drop-like) presentation, the atrophoderma of Pasini and Pierini, keloidal type, and the lichen sclerosis et atrophicus. Generalized morphea is defined as more than four indurated plaques larger than 3 cm and/or involving two or more corporal regions but sparing the face and hands. Linear morphea is the most common subtype in children and can present as "en coup de sabre" (ECDS), progressive hemifacial atrophy (Parry-Romberg syndrome [PRS]), or linear limb involvement. In these three subtypes the lesions progress rapidly to atrophy of the skin. ECDS can be associated with ocular and central nervous system involvement and usually presents on the paramedian forehead. Deep morphea involves the skin and deeper layers, such as muscle or bone. This type includes the morphea profunda that affect the subcutaneous tissue; eosinophilic fasciitis, which is a variant of deep morphea that affects the fascial plane; and pansclerotic morphea, that produces a circumferential involvement of the epidermis, dermis, subcutaneous tissue, muscle, and bone. The latter subtype elicits muscle atrophy, joint contractures, and non-healing ulcers. Patients with pansclerotic morphea and chronic wounds have been reported to present a high risk of squamous cell carcinoma of the skin. There is also a mixed variant of morphea composed by a combination of two or more subtypes [34, 35]. Histologically, the appearance of morphea can vary according with the phase of the disease. In the early stages, thickening of the collagen bundles, perivascular inflammatory infiltrates composed mainly of lymphocytes, plasma cells, and eosinophils can be detected. In the late stages, the inflammatory infiltrate regress and the dermal collagen bundles become more prominent and eosinophilic, and the eccrine glands, vessels, and subcutaneous fat become atrophic [34].

The activity of the disease can be monitored using sonography, therefore, the lesions can vary from hypoechogenicity and thickening of the dermis with hyperechogenicity of the subcutaneous tissue in the active phase, to thinning of the dermis and subcutaneous tissue in the atrophy phase. At the end stage (atrophy), a direct contact between the dermis and the muscle layer can be detected. Increased blood flow is commonly detected in the cutaneous layers during active phases. Nevertheless, the lesions become hypovascular on color Doppler imaging at the end stages. It is possible to detect the partial or full thickness involvement of the lesions and their asynchronic presentation using sonography (i.e., multiple lesions in different phases of activity). The most sensitive sonographic signs for detecting activity are cutaneous hypervascularity and increased echogenicity of the underlying subcutaneous tissue (100 % sensitivity and specificity for both). In patients that present with PRS (progressive hemifacial atrophy), the ipisilateral parotid gland has been reported to be affected with signs of inflammation [35–38] (Figs. 4.23, 4.24, 4.25, 4.26, 4.27, 4.28 and 4.29).

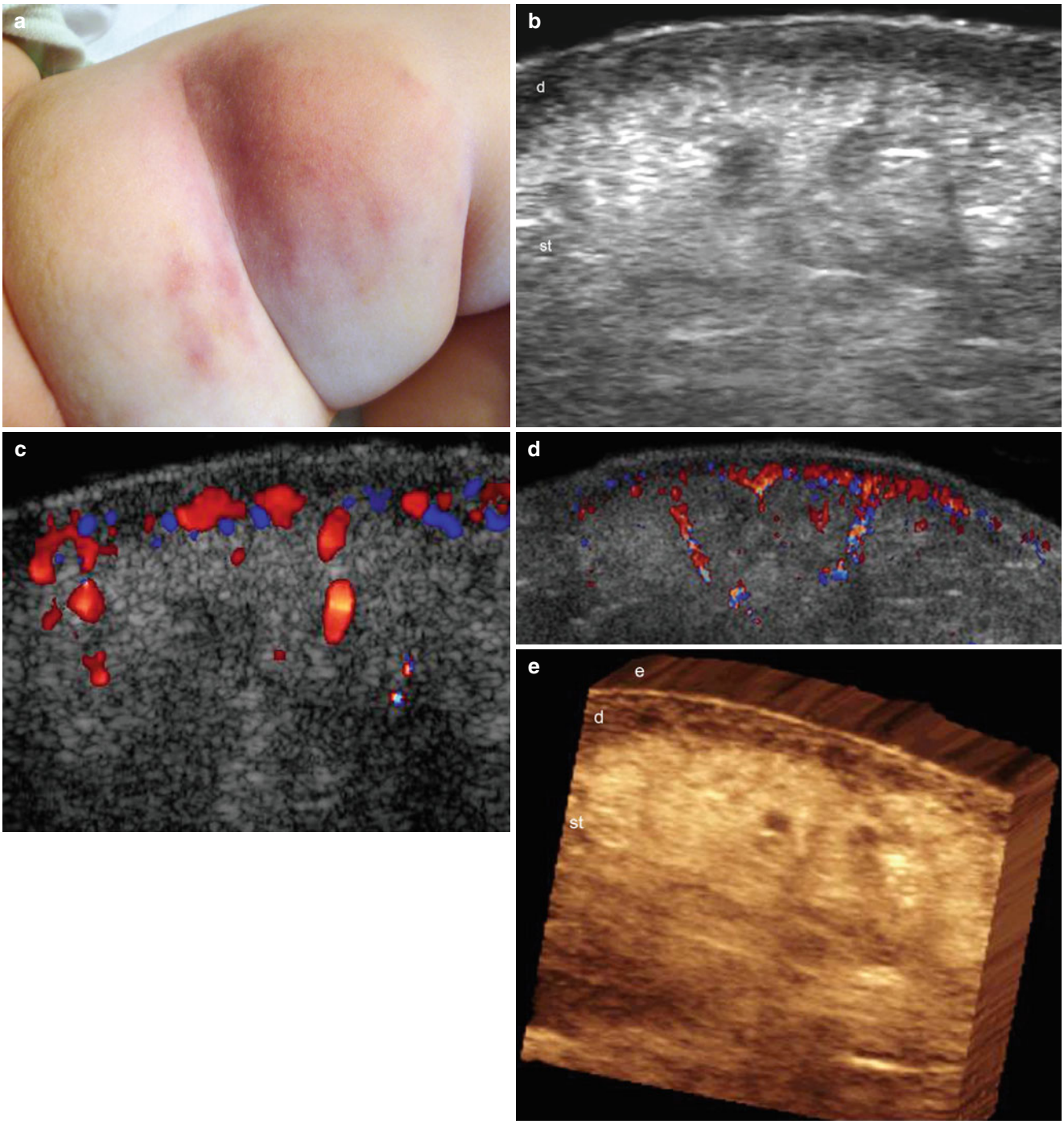

Fig. 4.23 (**a**–**e**) Active morphea (inflammatory phase). (**a**) Clinical erythematous swelling in the left thigh of an infant. (**b**) Gray scale ultrasound image (transverse view) shows thickening and decreased echogenicity of the dermis and increased echogenicity of the subcutaneous tissue. (**c**) Color Doppler ultrasound image (transverse view) demonstrates increased blood flow in the dermis and upper subcutaneous tissue. (**d**) Color Doppler ultrasound image (extended field transverse view) of the lesional area. (**e**) The lesion in 3D (5–8 s sweep). *Abbreviations*: *e* epidermis, *d* dermis, *st* subcutaneous tissue

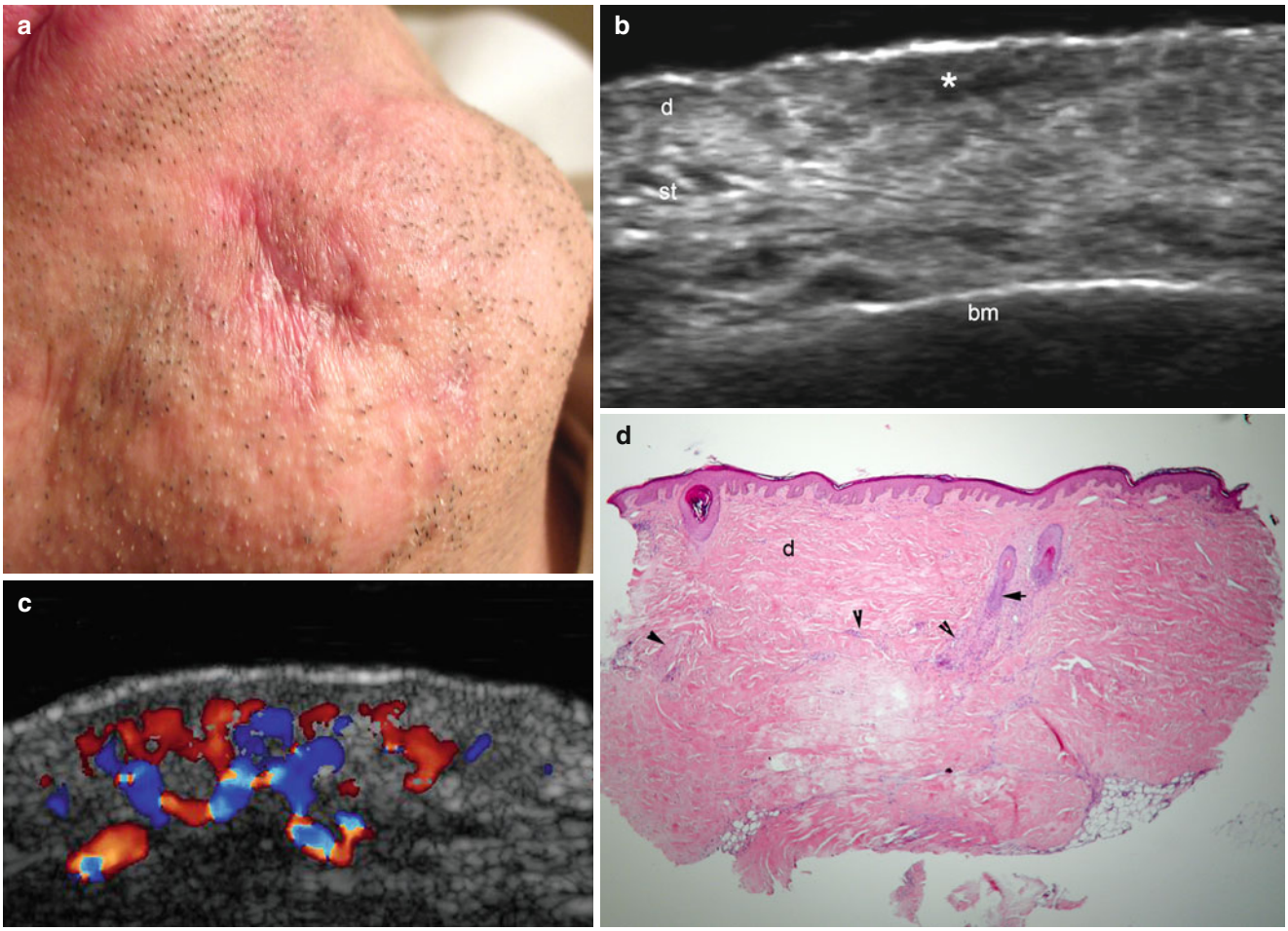

Fig. 4.24 (**a**–**d**) Active morphea (inflammatory phase). (**a**) Clinical lesion shows erythema, swelling and retraction in the chin. (**b**) Gray scale ultrasound image (transverse view) demonstrates thickening and decreased echogenicity of the dermis (*) and increased echogenicity of the subcutaneous tissue. (**c**) Color Doppler ultrasound image (transverse view) shows increased vascularity in the dermis and upper subcutaneous tissue. (**d**) Histology (HE 20 × zoom) illustrates the thick collagen bundles in the dermis (*d*) and the inflammatory infiltrates (*arrowheads*). There is also atrophy of the adnexal structures (*arrow*; i.e., hair follicles and perifollicular glands). *Abbreviations*: *d* dermis, *st* subcutaneous tissue, *bm* bony margin of the mandible

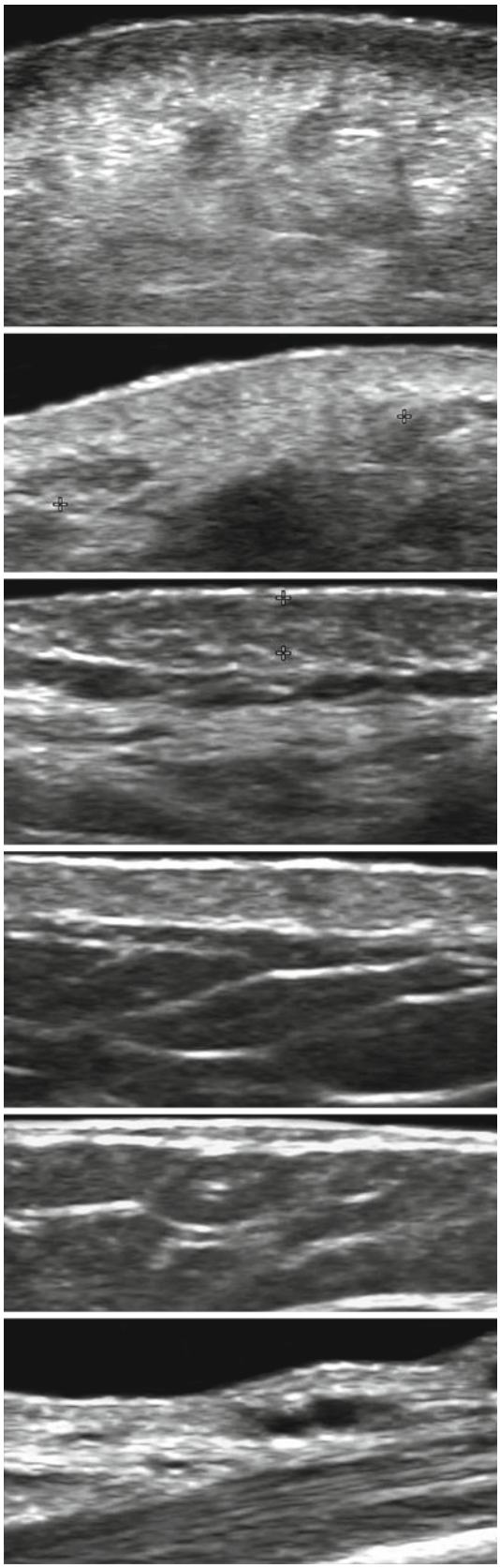

Fig. 4.25 Grading of activity in morphea (grey scale) going from active (*top*) to atrophy (*bottom*) phases

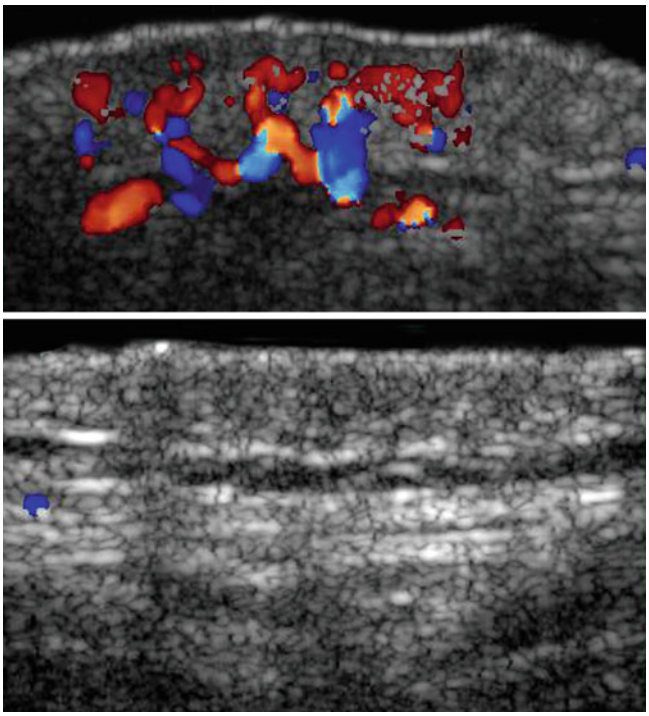

Fig. 4.26 Grading of activity in morphea (color Doppler ultrasound image) going from active (*top*, hypervascular) to atrophy (*bottom*, hypovascular) phases

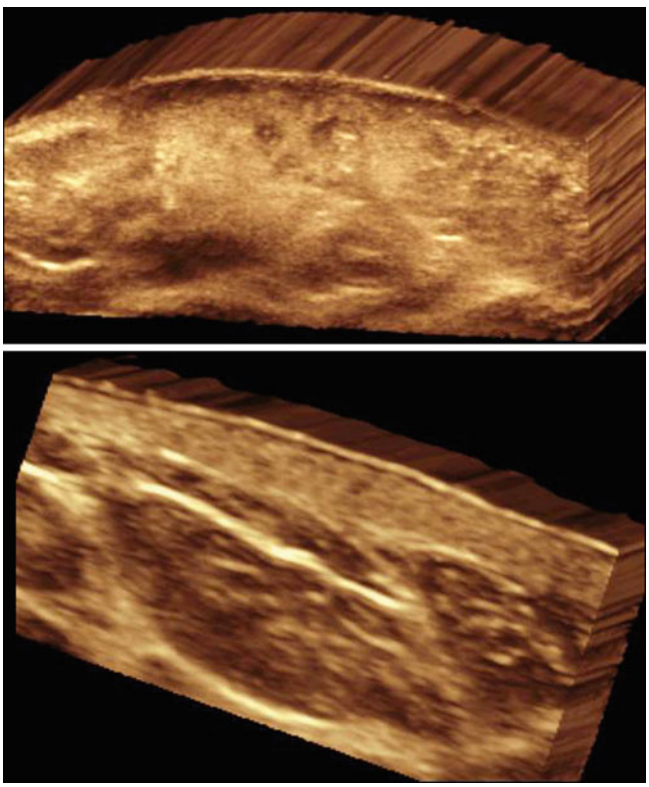

Fig. 4.27 Grading of activity in morphea (3D reconstructions) going from active (*top*) to inactive (*bottom*)

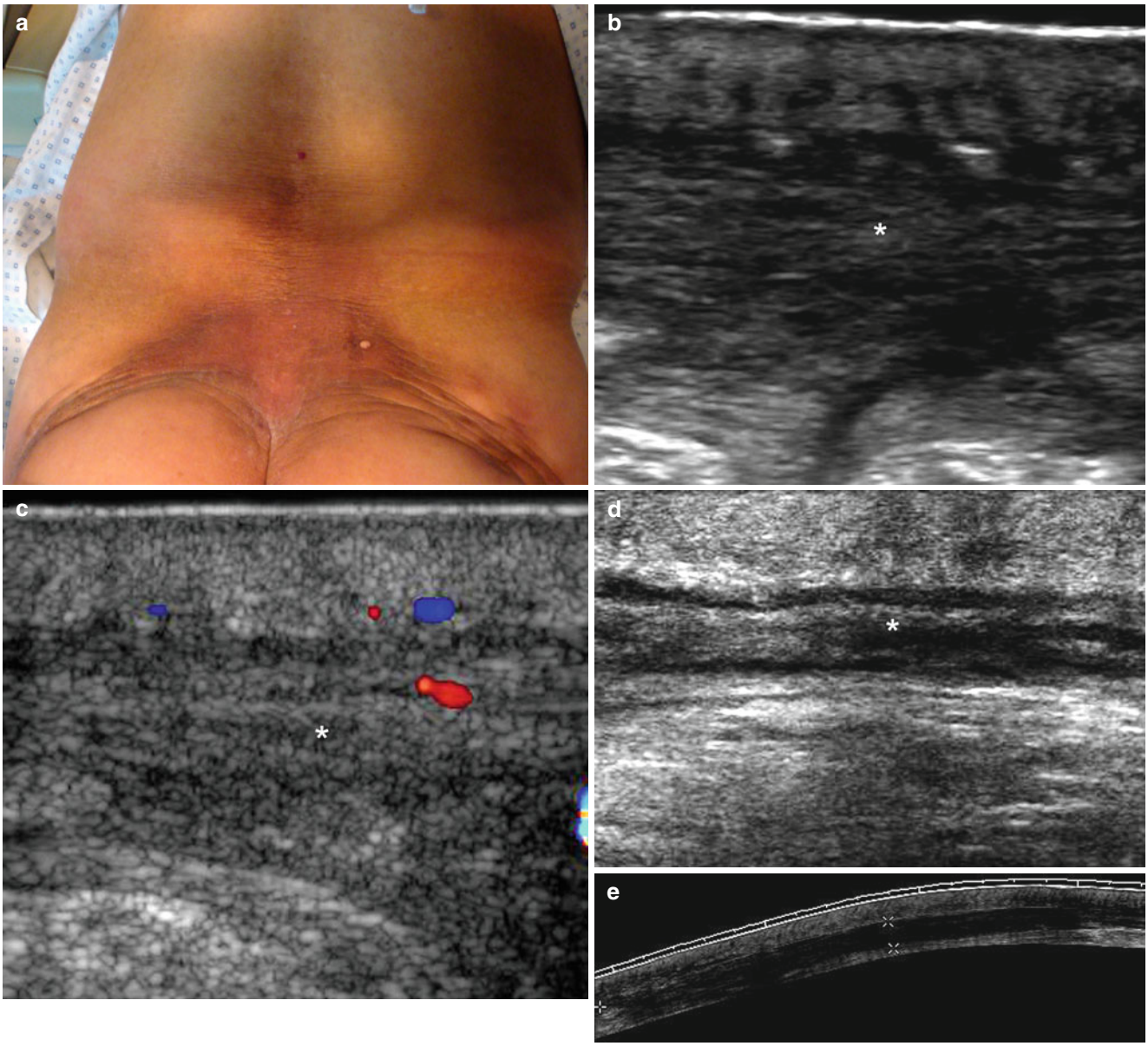

Fig. 4.28 (**a**–**e**) Deep morphea-eosinophilic fasciitis. (**a**) Clinical lesion shows hyperpigmented and indurated plaque in the lumbar and gluteal region. (**b**) Gray scale ultrasound image (transverse view) demonstrates increased thickening and decreased echogenicity of the fascial plane (*). There is also decreased echogenicity and thickening of the dermis. (**c**) Color Doppler ultrasound image (transverse view) shows increased blood flow in the lower dermis and fascial layer (*). (**d**) Gray scale ultrasound image (transverse view) depicts the decreased echogenicity and thickening of the fascia (*). (**e**) Gray scale (extended field of view, transverse axis) shows the wide extension of the lesion that involves the fascial layer (between markers)

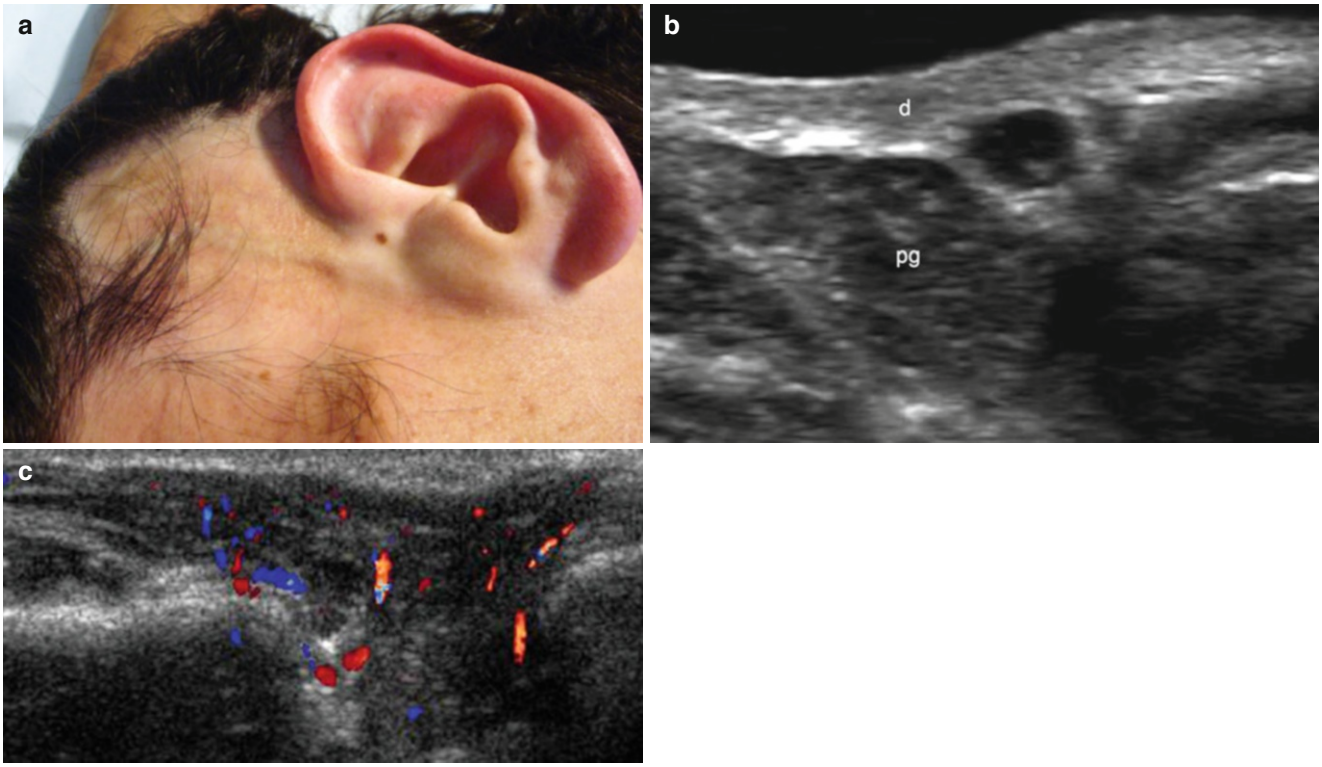

Fig. 4.29 (**a**–**c**) Morphea at the phase of atrophy (Parry-Romberg syndrome). (**a**) Clinical image shows atrophy of the left side of the face and baldness in the regional scalp. (**b**) Gray scale ultrasound image (transverse view at the left cheek) demonstrates lack of fat in the subcutaneous tissue and decreased echogenicity of the dermis (*d*). The underlying parotid gland (*pg*) presents hypoechogenicity. (**c**) Color Doppler ultrasound image (transverse view) shows hypoechogenicity and increased vascularity in the left parotid gland

4.2.11 Cutaneous Lupus

Cutaneous lupus is the cutaneous form of lupus erythematous (LE) and may precede systemic involvement. The term 'cutaneous lupus erythematosus' (CLE) comprises several related autoimmune skin disorders, defined as 'specific' skin manifestations of LE. The spectrum of clinical presentation of CLE is wide, reaching from mild erythema to disseminated scarring skin lesions, all of them photosensitive dermatosis [39]. According to the phase of activity and presentation of the disease, there are three forms of cutaneous lupus: acute cutaneous lupus (classical malar erythematous eruption with a butterfly pattern in the midface and/or a generalized erythematous maculopapular eruption), subacute cutaneous lupus (non-scarring, non–atrophy-producing), and chronic cutaneous (discoid) lupus (scarring, atrophy producing) [40]. Nonspecific skin lesions such as generalized or acrolocalized (i.e., peripheral location such as limbs, fingers, or ears) vasculitis, livedo reticularis, and alopecia are frequently seen in patients with cutaneous lupus. Other typical cutaneous lupus subsets, such as lupus profundus/panniculitis, lupus tumidus, urticaria vasculitis, hypertrophic lupus, and bullous lupus are rather rare variants. Butterfly rash and/or macular exanthema are characteristic skin lesions of systemic LE rarely found in patients with cutaneous lupus [41]. It is the localized cutaneous form of lupus characterized by erythematous plaques or swellings that can evolve to atrophic or depigmented plaques at the end stage. Histologically, lupus presents mucin deposits, thick collagen, and inflammatory cells according to the stage of the disease.

On sonography, active cutaneous lupus shows hypoechogenicity and thickening of the dermis and increased echogenicity of the subcutaneous tissue. The hypoechogenicity of the dermis tends to adopt a fusiform shape. Lesional hypervascularity is commonly detected in active stages. Atrophy of the cutaneous layers and hypovascularity are common at the end stages (discoid lupus). Information about the involvement of vessels, such as the digital arteries, can be obtained. These vessels can present thrombotic and vasculitis phenomena, which can complicate the treatment and/or prognosis of the disease. These thromboses present as hypoechoic filling of the vessels using sonography. Absence of flow is demonstrated on the spectral curve analysis on color Doppler ultrasound [22, 42, 43] (Figs. 4.30, 4.31, 4.32, 4.33 and 4.34).

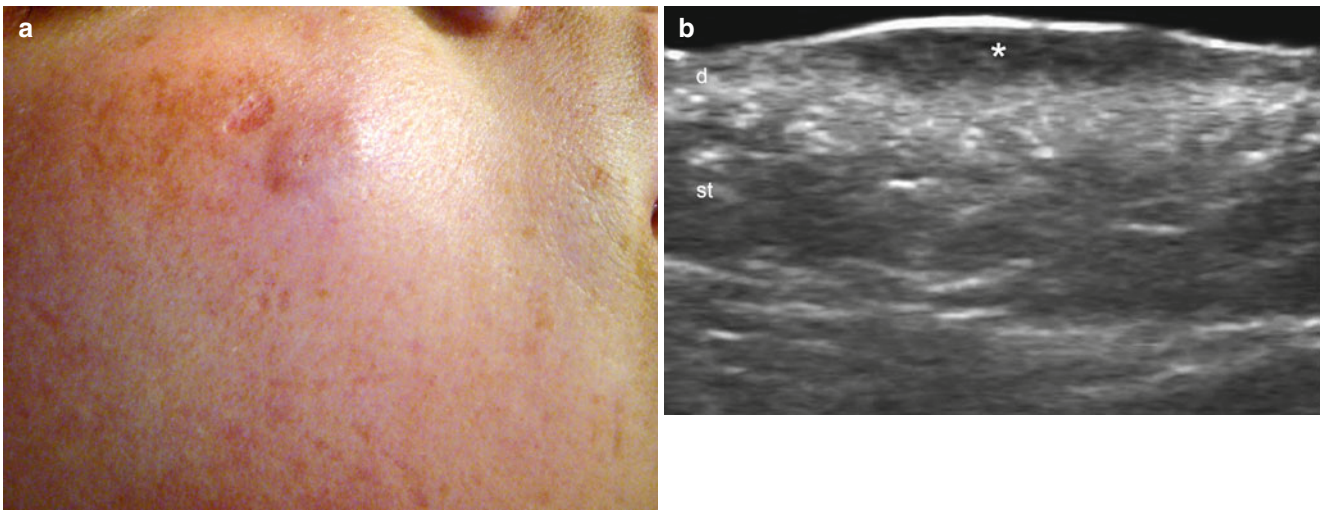

Fig. 4.30 (**a**–**e**) Cutaneous lupus (active phase) (**a**) Clinical image shows erythematous swelling in the right cheek. (**b**) Gray scale ultrasound image (transverse view) demonstrates fusiform-shaped thickening and decreased echogenicity of the upper dermis (*). There is also increased echogenicity of the lower dermis and upper subcutaneous tissue. (**c**) Color Doppler ultrasound image (transverse view) shows increased vascularity in dermis and subcutaneous tissue. (**d**) Histology (HE × 20 zoom) demonstrates interface vacuolar alterations, extensive perivascular and periadnexial inflammatory reaction, and mucin deposits. (**e**) (Alcian Blue ×100 zoom) shows prominent mucin deposition (*blue color*) in dermis between the collagen bundles. *Abbreviations*: *d* dermis, *st* subcutaneous tissue

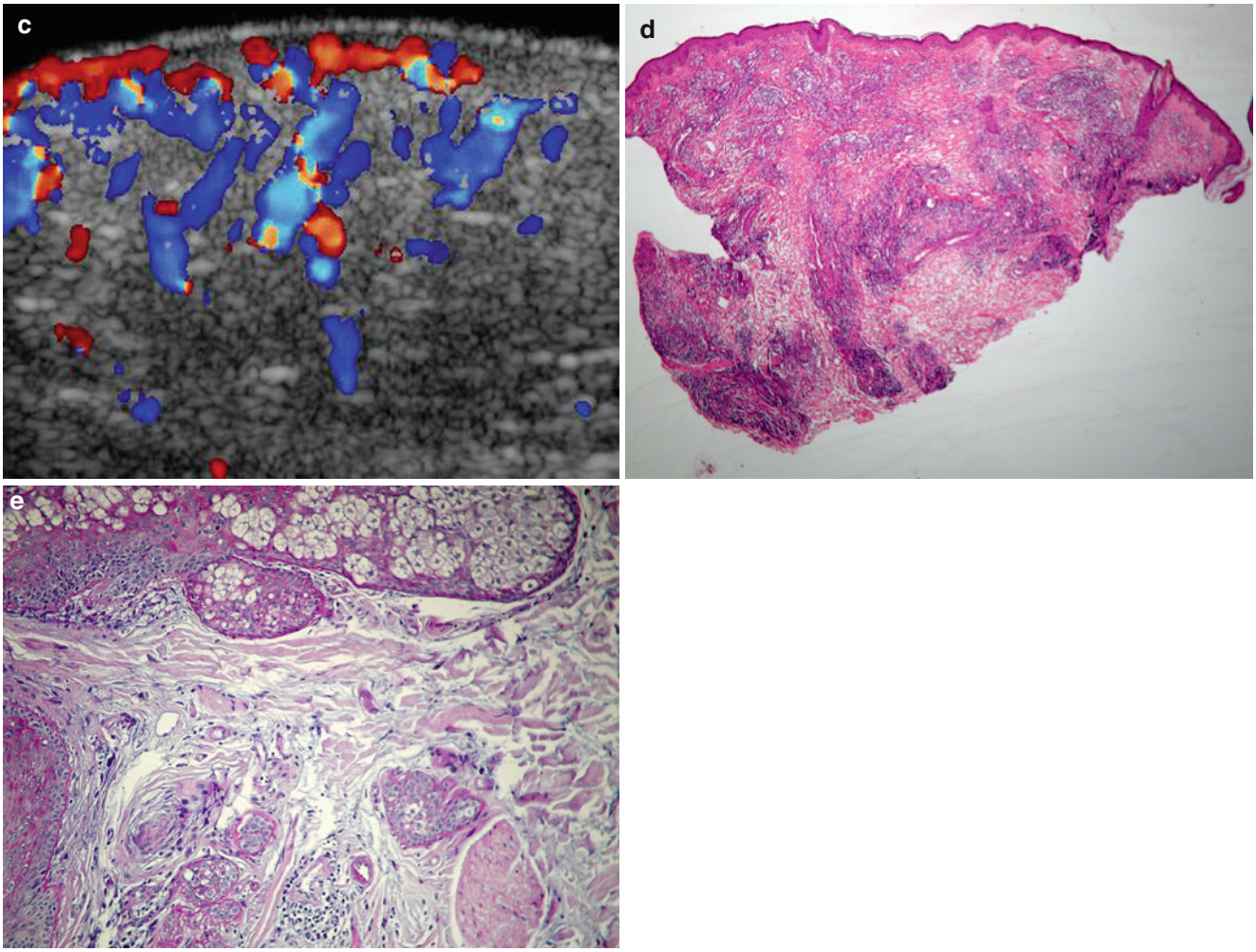

Fig. 4.30 (continued)

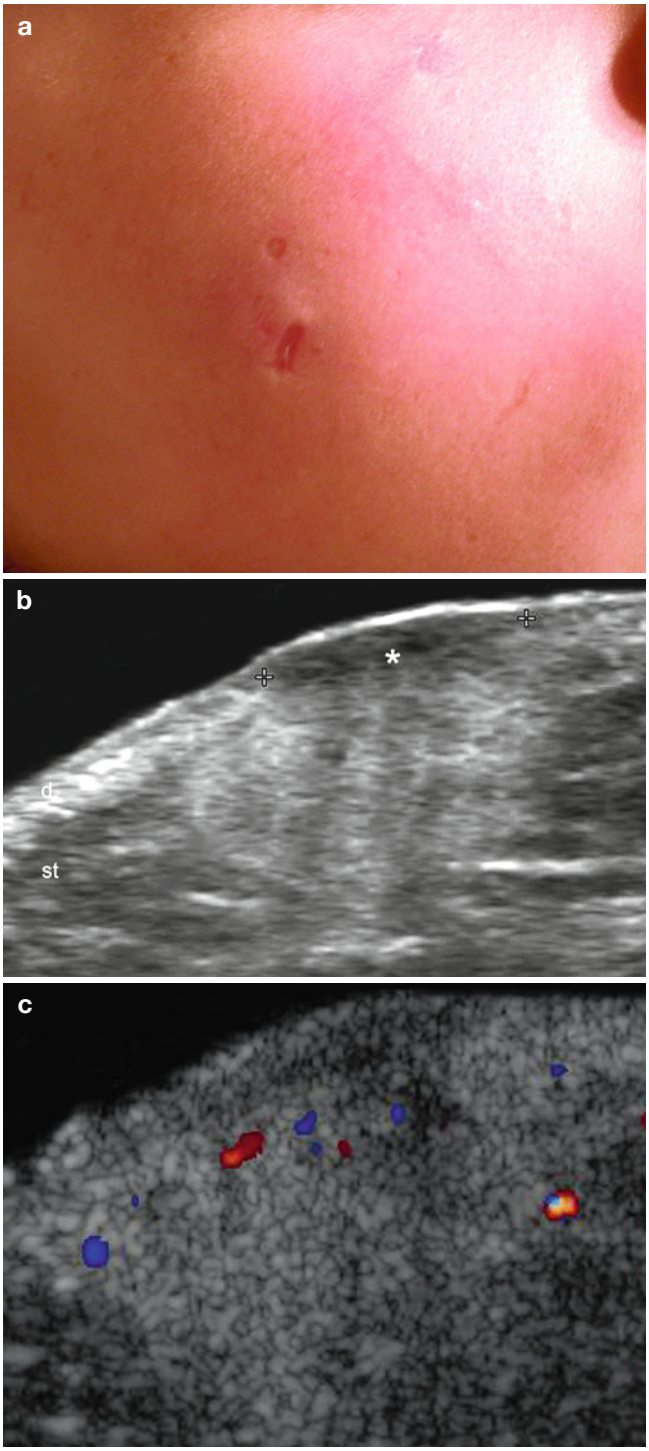

Fig. 4.31 (**a**–**c**) Cutaneous lupus (active phase). (**a**) Clinical image with erythema and swelling in the right cheek. (**b**) Gray scale ultrasound image (transverse view) shows fusiform shaped decreased echogenicity and thickening of the dermis (*) as well as increased echogenicity of the subcutaneous tissue. (**c**) Color Doppler ultrasound image (transverse view) demonstrates increased vascularity in the lesional site. *Abbreviations*: *d* dermis, *st* subcutaneous tissue

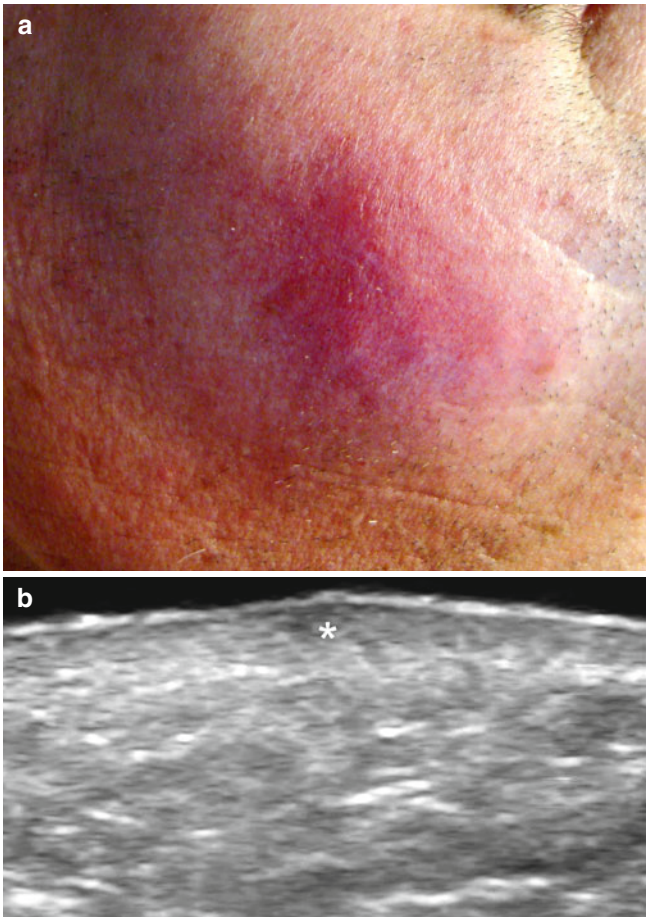

Fig. 4.32 (**a**, **b**) Cutaneous lupus (active phase). (**a**) Clinical image demonstrates erythema and swelling in the right cheek. (**b**) Gray scale ultrasound image (transverse view) shows thickening and decreased echogenicity of the dermis (*). Increased echogenicity of the upper subcutaneous tissue is also detected

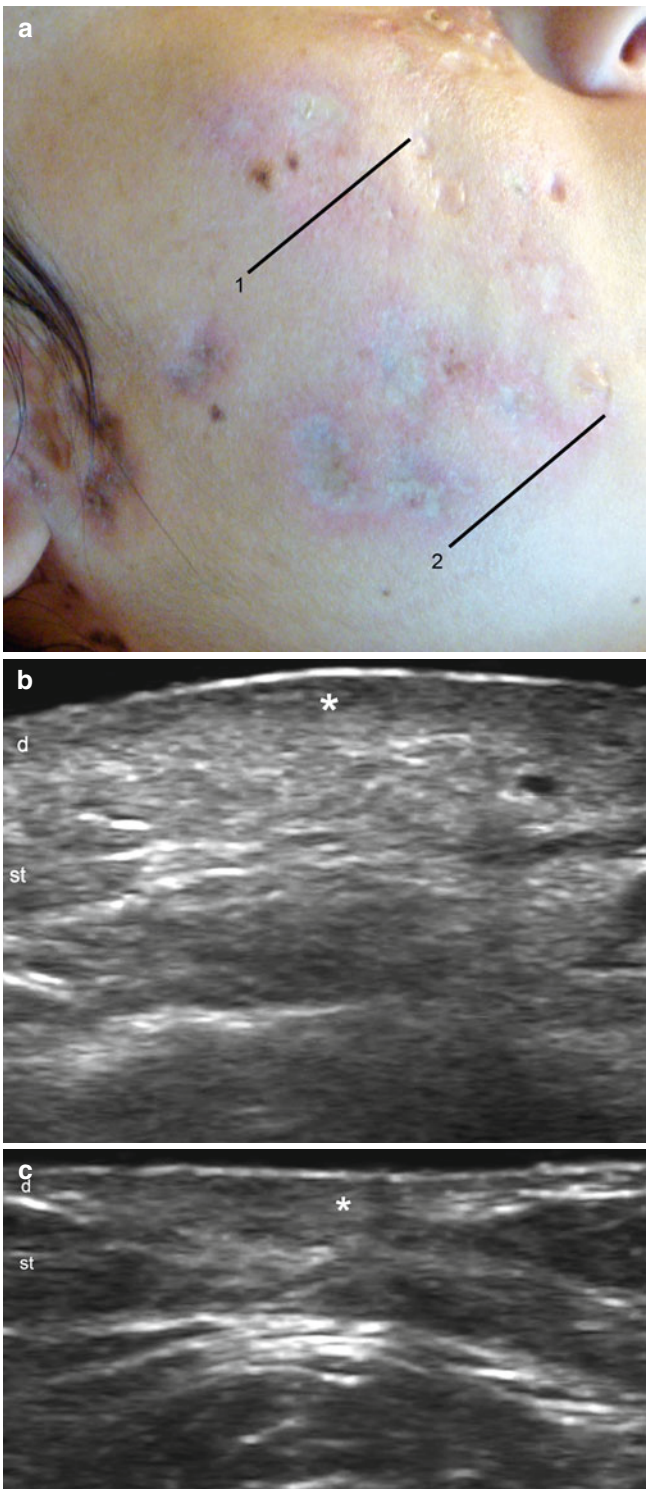

Fig. 4.33 (**a**–**c**) Discoid cutaneous lupus. (**a**) Clinical image shows disk shaped erythematous lesions and scarring in the right cheek. The *black lines* illustrate the level and orientation of the following ultrasound views. (**b**) Gray scale ultrasound image (transverse view, level 1) shows decreased echogenicity of the upper dermis (*) and increased echogenicity of the lower dermis and subcutaneous tissue. (**c**) Gray scale ultrasound image (transverse view) shows thickening and decreased echogenicity of the dermis (*). Increased echogenicity and lack of fatty lobules in the subcutaneous tissue is also detected. *Abbreviations*: *d* dermis, *st* subcutaneous tissue

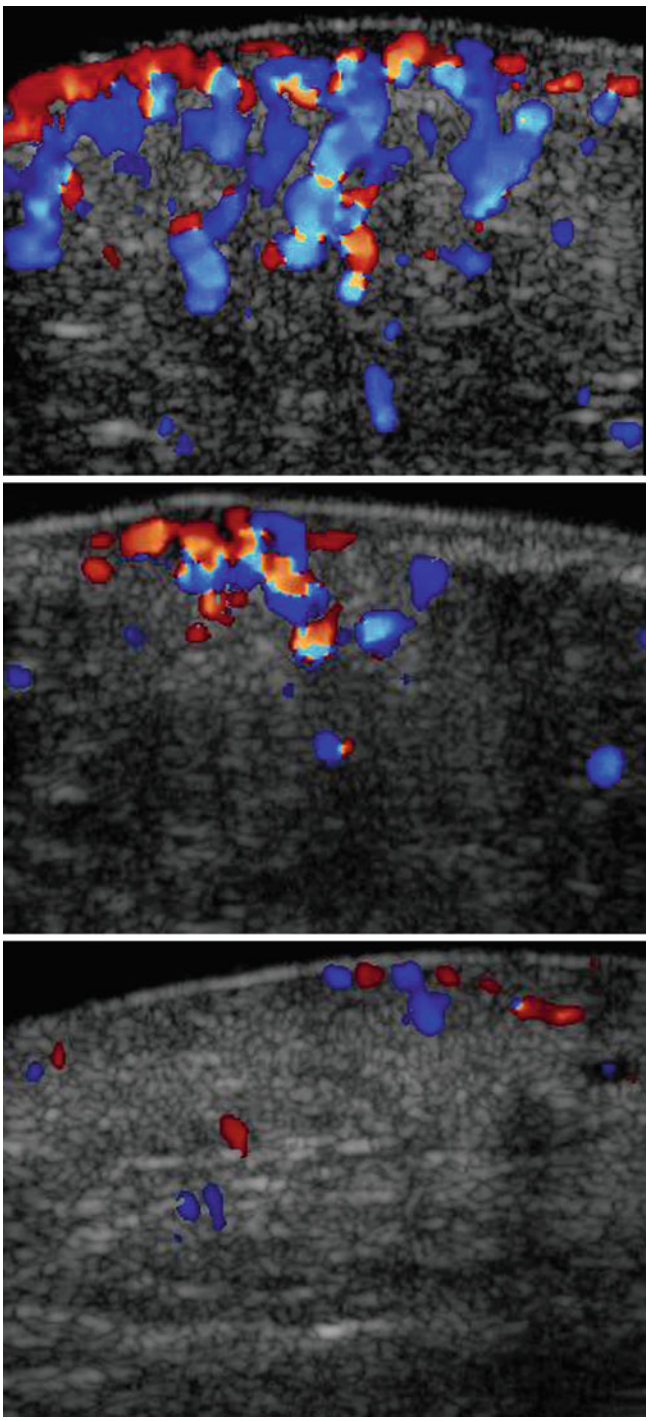

Fig. 4.34 Grading of vascularity in cutaneous lupus going from hypervascular (*top*) to hypovascular (*bottom*)

4.2.12 Dermatomyositis

Dermatomyositis is a systemic autoimmune disease that primarily affects skeletal muscle, skin, and the lungs. Although the disorder is rare, with a prevalence of one to ten cases per million in adults and one to 3.2 cases per million in children, early recognition and treatment are important ways to decrease the morbidity of systemic complications. Dermatomyositis is characterized by autoantibodies, tissue inflammation, parenchymal cell damage and death, and vasculopathy. Clinically, these patients present with "Gottron's papules" (erythematous, usually symmetric and keratotic macules located over the methacarpal and interphalangeal joints that can mimic psoriasis), "heliotrope rash" (violaceous eruption on the upper eyelids and rarely on the lower eyelids), the shawl sign (erythematous, poikilodermatous macules distributed in a "shawl" pattern over the shoulders, arms, and upper back), the V-sign (erythematous eruption in a V-shaped distribution over the anterior neck and chest), and periungual telangiectasias. Calcinosis is usually subclinical, although when the deposits are large, they can be palpable as an induration and associated to hyperpigmentation. Proximal muscle weakness or pain (upper or lower extremity and trunk) and elevated serum creatine kinase or aldolase levels are common. The diagnosis is confirmed by histology that shows a mixed B- and T-cell perivascular inflammatory infiltrate and perifascicular muscular fiber atrophy on the muscle biopsy.

Increased echogenicity of the muscle secondary to edema can be detected on sonography. Contrast-enhanced ultrasound with its capability of measuring perfusion has been reported as a useful tool for diagnosing acute inflammation in poly- and dermatomyositis. Calcinosis can be also detected on sonography and presents as hyperechoic spots, usually with posterior acoustic shadowing. Increased echogenicity of the subcutaneous tissue secondary to panniculitis has also been reported [22, 44–47] (Figs. 4.35 and 4.36).

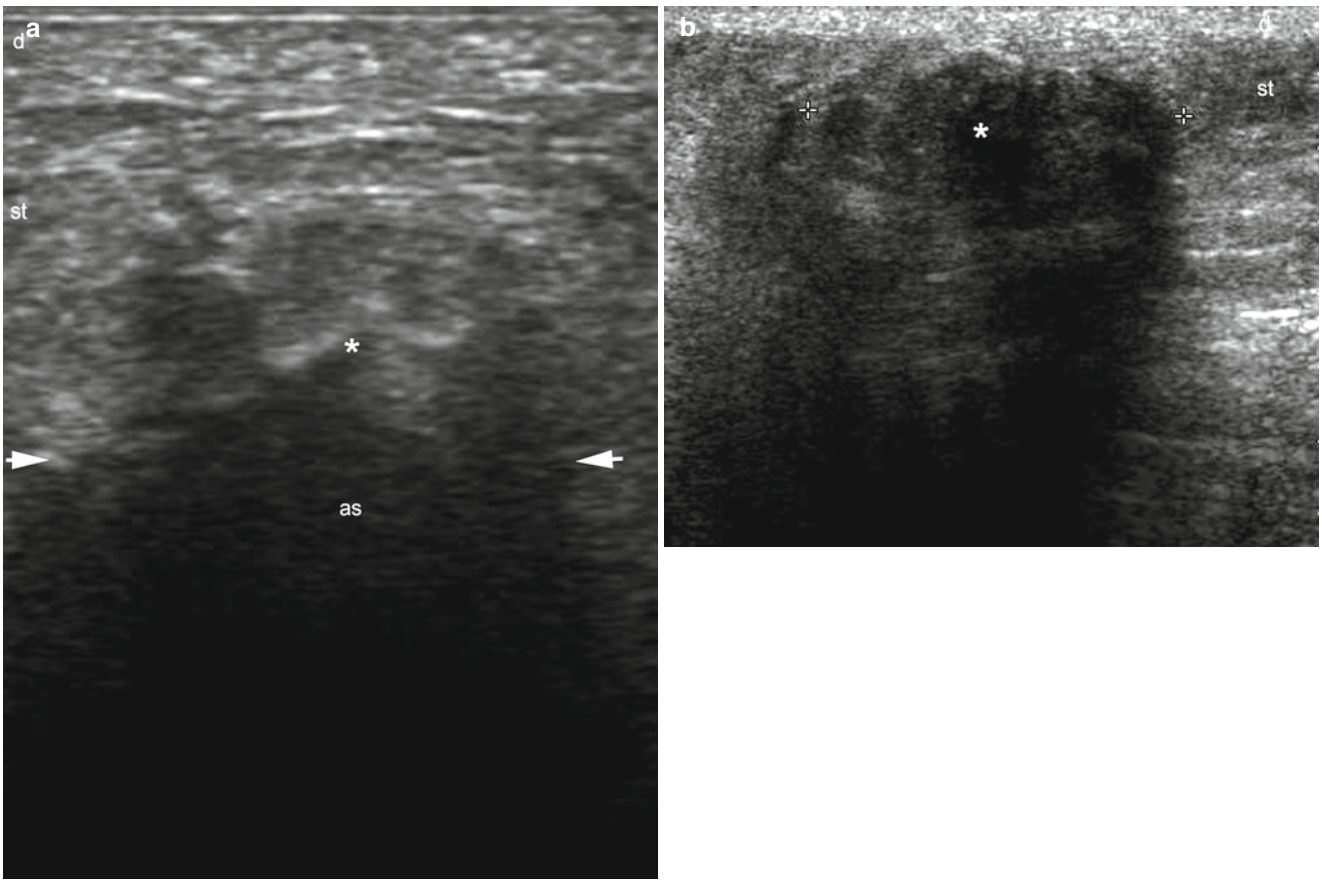

Fig. 4.35 (**a**, **b**) Calcinosis in dermatomyositis. (**a**, **b**) Gray scale ultrasound images (**a**: transverse view, left hip region and **b**: longitudinal view, left gluteal region) show hyperechoic deposits (*) in the subcutaneous tissue that generates strong posterior acoustic shadowing artifact (as, *arrows* (a) and markers (b)). *Abbreviations*: *d* dermis, *st* subcutaneous tissue

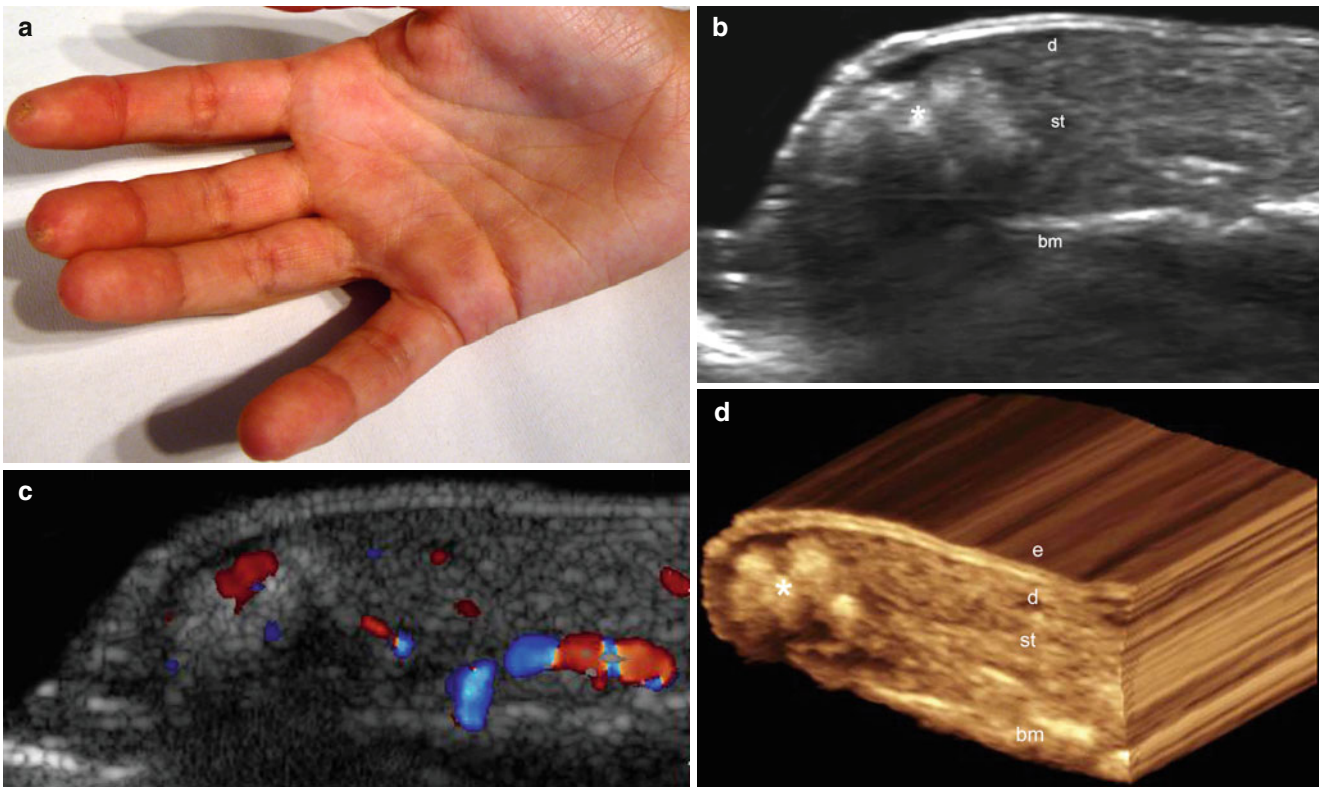

Fig. 4.36 (**a**–**d**) Calcinosis in dermatomyositis. (**a**) Clinical image shows bumps in the tip of the right index and middle fingers. (**b**) Gray scale ultrasound image (longitudinal view, index finger) demonstrates hyperechoic calcium deposits (*) in dermis and subcutaneous tissue. There is also hypoechogenicity of the upper dermis suggestive of inflammation and posterior acoustic shadowing artifact. (**c**) Color Doppler ultrasound image (longitudinal view, index finger) shows increased vascularity in the periphery of the calcium deposits. (**d**) The calcium deposits (*) in 3D (5–8 s, longitudinal reconstruction). *Abbreviations*: *e* epidermis, *d* dermis, *st* subcutaneous tissue, *bm* bony margin of the distal phalanx

4.2.13 Hidradenitis Suppurativa

Hidradenitis suppurativa (HS), also called acne inversa, is a chronic and recurrent inflammatory disease affecting the skin that bears prominent hair follicles and apocrine glands. The exact cause is still controversial but seems to present an autoimmune origin. Clinically, HS shows painful, deep seated inflamed lesions including nodules, sinus tracts, and abscesses with scarring and inflammation in the axillae and groin regions. This disease can less commonly affect the buttock, vulvar, or inframammary regions. The severity of the disease can be clinically assessed using Hurley's classification that separates the stages in: I mild, II moderate and III severe [48]. Histology shows follicular occlusion and inflammatory involvement of the apocrine glands with dense lymphocytic infiltrates around the hair follicle, and acute and chronic inflammatory cells around the apocrine glands. The inflamed sinus tracts frequently contain desquamated keratin, histiocytes, giant cells, and hair shafts within dense fibrosis. Squamous epithelium lined cyst or sinuses in the dermis all containing keratin and containing half hair shafts are usually observed [49]. On sonography, anechoic fluid collections with echoes (debris) and fragments of hair shafts, hypoechoic fistulous tracts in the dermis and subcutaneous tissue, thickening and hypoechogenicity of the dermis, and enlargement of the hair follicles can be detected. Frequently increased vascularity is observed in the periphery of the collections and regional lymph nodes seem to conserve the size, although they may present some cortical thickening during the inflammatory phases. Additionally, anechoic or hypoechoic dermal pseudocystic subclinical lesions in the dermis can be seen [50, 51]. Sonography may support the diagnosis and the assessment of severity in this recurrent disease [52] (Figs. 4.37, 4.38, 4.39, 4.40, 4.41, 4.42, 4.43 and 4.44).

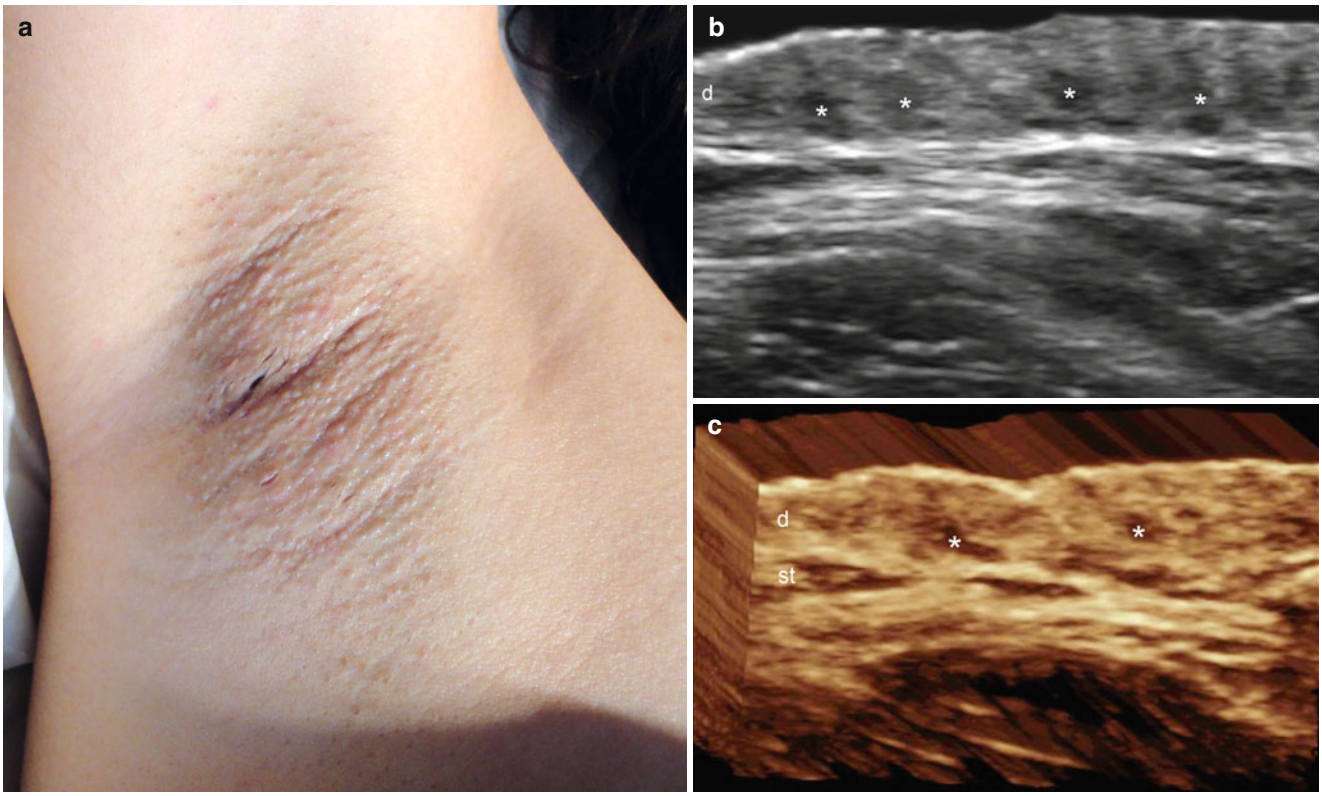

Fig. 4.37 (**a**–**c**) Hidradenitis suppurativa. (**a**) Clinical image shows erythema in the right axilla (Hurley I). (**b**) Gray scale ultrasound image (transverse view) demonstrates enlargement of the base of the hair follicles (*), decreased echogenicity and thickening of the dermis. (**c**) The lesional area in 3D (transverse view, 5–8 s reconstruction). *Abbreviations*: *d* dermis, *st* subcutaneous tissue

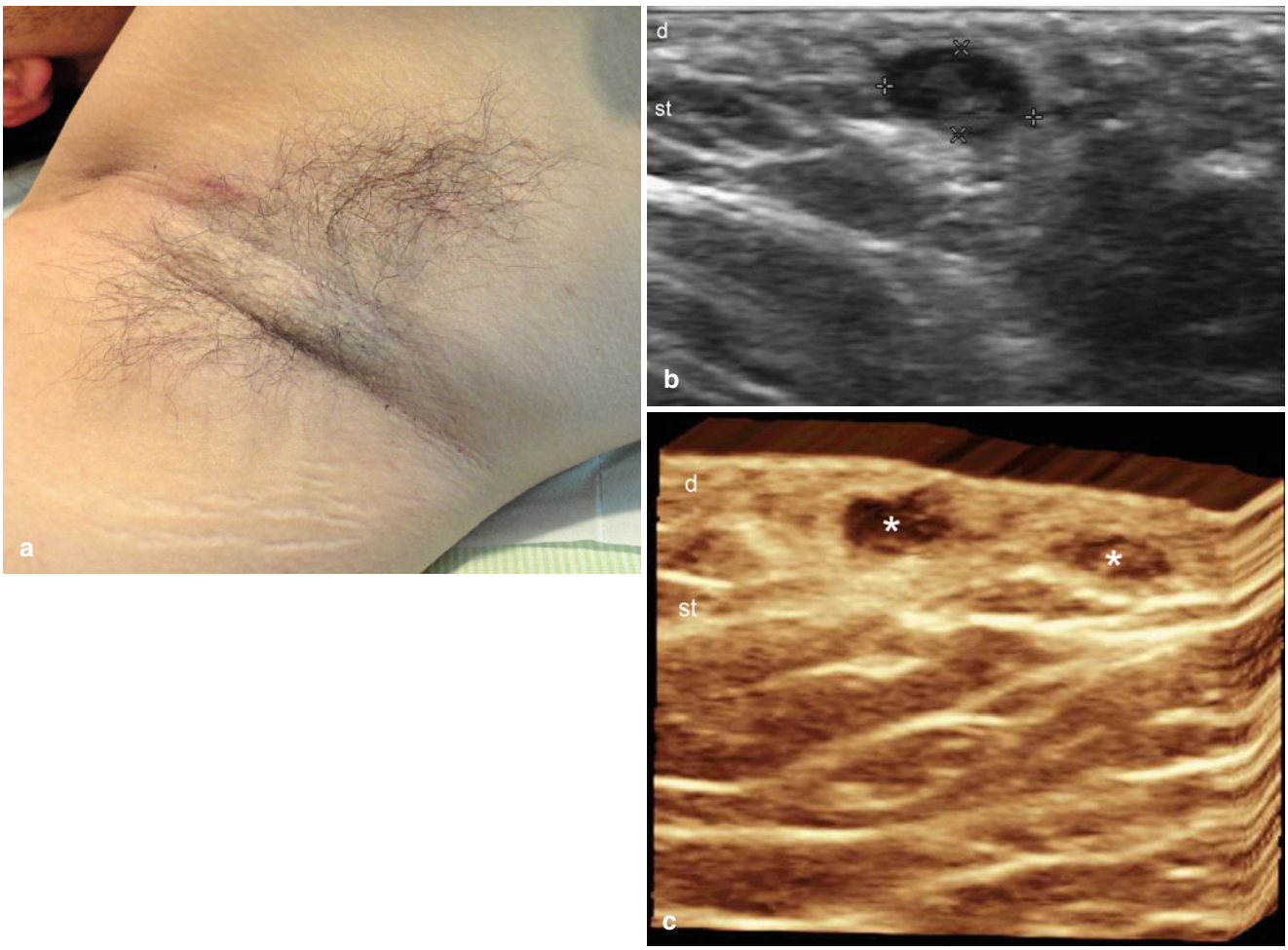

Fig. 4.38 (**a**–**c**) Hidradenitis suppurativa. (**a**) Clinical image shows patchy erythematous areas in the right axilla (Hurley I). (**b**) Gray scale ultrasound image (transverse view) demonstrates hypoechoic oval shaped pseudocystic structure (between markers) in the dermis and upper subcutaneous tissue. (**c**) 3D reconstruction (5–8 s reconstruction, transverse axis) depicts two hypoechoic round shaped pseudocystic lesions (*) in the dermis. *Abbreviations*: *d* dermis, *st* subcutaneous tissue

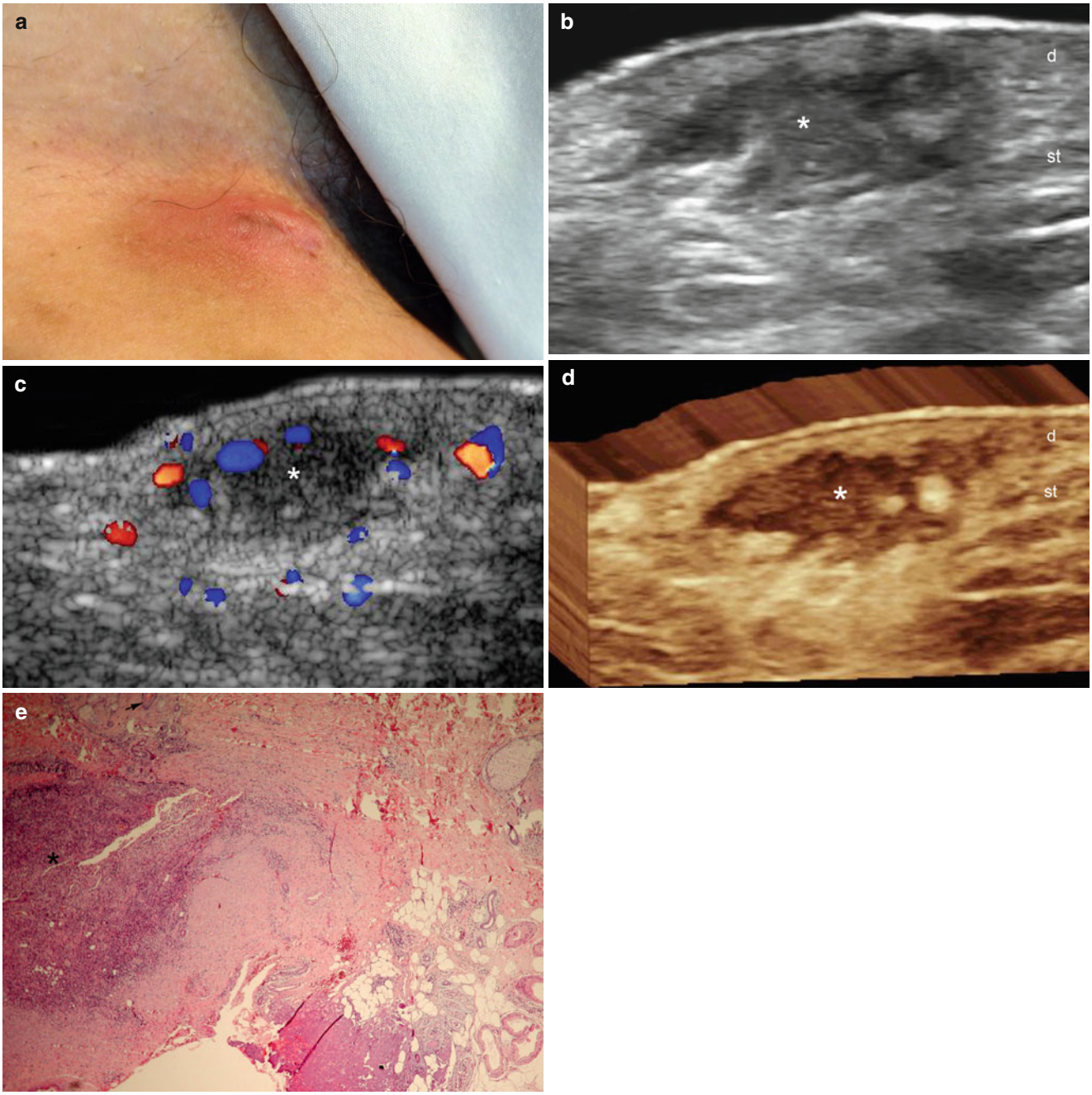

Fig. 4.39 (**a**–**e**) Hidradenitis suppurativa. (**a**) Clinical image shows erythematous swelling in the right groin (Hurley II). (**b**) Gray scale ultrasound image (transverse view) demonstrates hypoechoic collection (*) with echoes (debris) and irregular borders in the dermis and subcutaneous tissue that connects to the base of the hair follicles. Thickening and decreased echogenicity of the dermis is also detected. (**c**) Color Doppler ultrasound image (transverse view) shows increased vascularity in the periphery of the collection (*). (**d**) The collection (*) in 3D (5–8 s sweep reconstruction). (**e**) Histology (HE × 100 zoom) depicts a suppurative inflammatory reaction with polymorphonuclear cells and fibrosis (*). The base of a hair follicle is detected in the upper part of the figure (*arrow*). Adipose cells and apocrine glands are shown in the right side of the image (*bottom*). *Abbreviations*: *d* dermis, *st* subcutaneous tissue

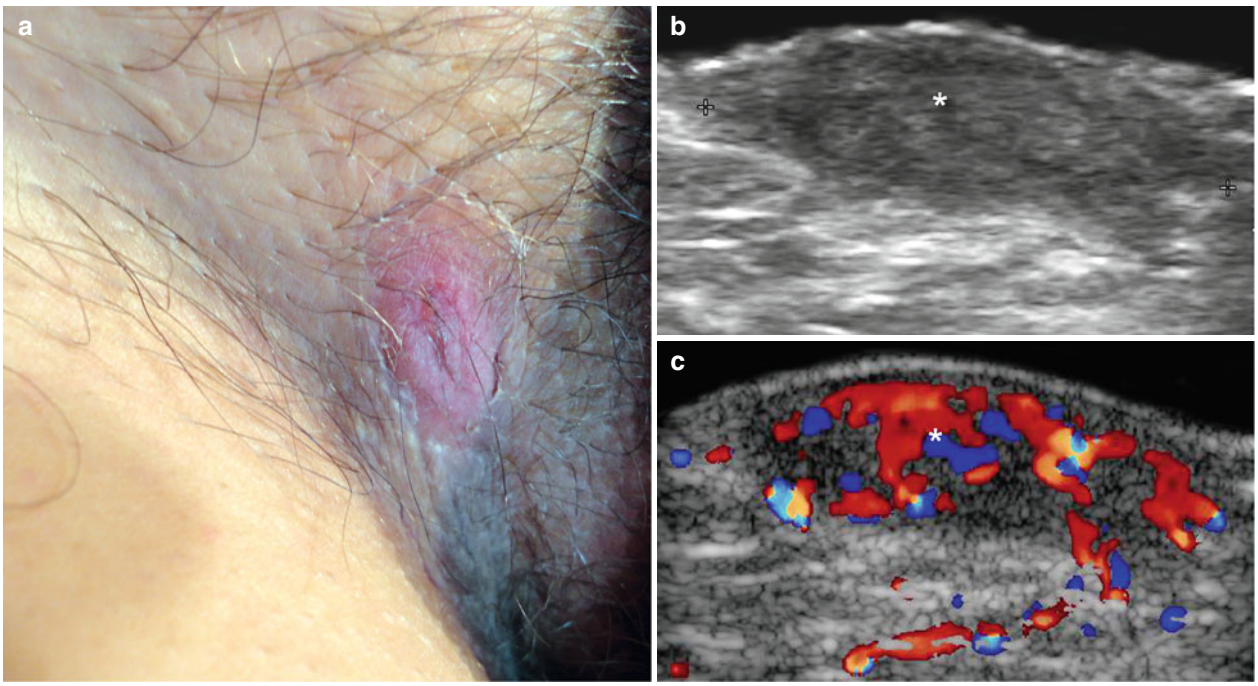

Fig. 4.40 (**a**–**c**) Hidradenitis suppurativa. (**a**) Clinical image shows erythematous bump in the right groin (Hurley I). (**b**) Gray scale ultrasound image (transverse view) demonstrates hypoechoic fluid collection with prominent echoes (debris and inflammatory/granulomatous tissue) (*, between markers) in the dermis and upper subcutaneous tissue. (**c**) Color Doppler ultrasound image (transverse view) shows increased blood flow in the collection

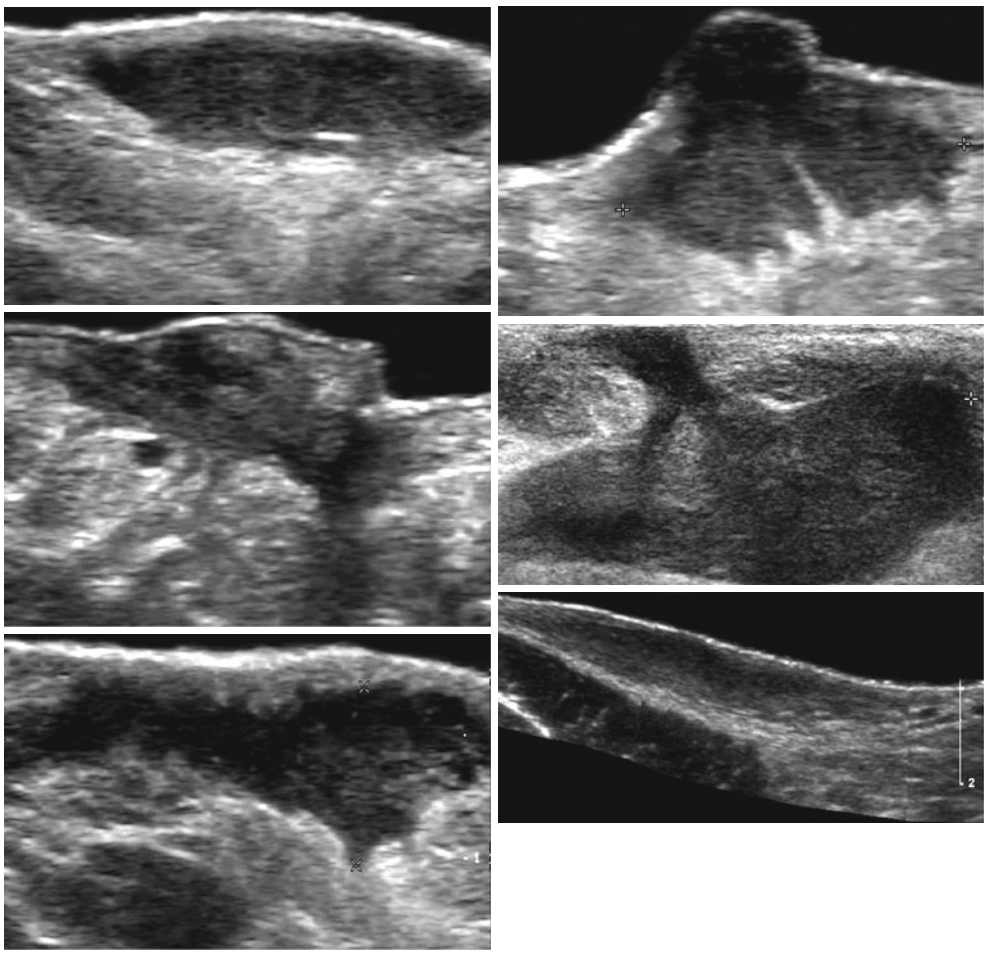

Fig. 4.41 Variable appearance of the fluid collections in hidradenitis suppurativa

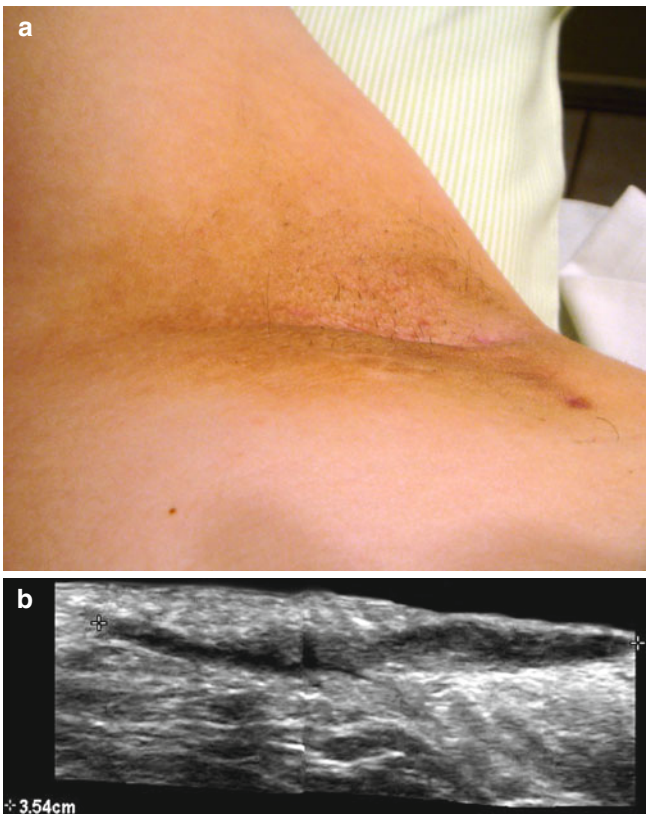

Fig. 4.42 (**a**, **b**) Hidradenitis suppurativa. (**a**) Clinical image shows slight erythema and retraction in the left axilla (Hurley I). (**b**) Gray scale ultrasound image (longitudinal view) depicts 3.54 cm hypoechoic fistulous tract (between markers) running in the dermis and upper subcutaneous tissue

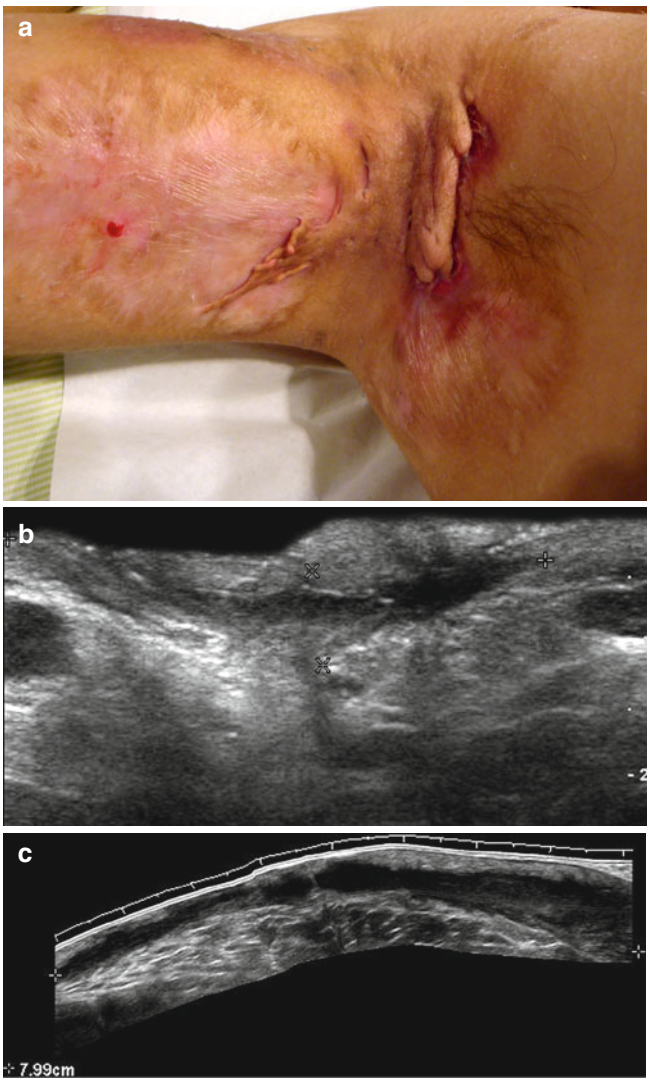

Fig. 4.43 (**a**–**c**) Hidradenitis suppurativa. (**a**) Clinical image shows extensive scarring, erythema and bumps in the right axilla (Hurley III). (**b**) Gray scale ultrasound image (transverse view) demonstrates one of the several hypoechoic fistulous tracts (between markers). (**c**) Gray scale extended field of view (longitudinal view) shows a 7.99 cm long hypoechoic fistulous tract (between markers) located in dermis and subcutaneous tissue in the same patient

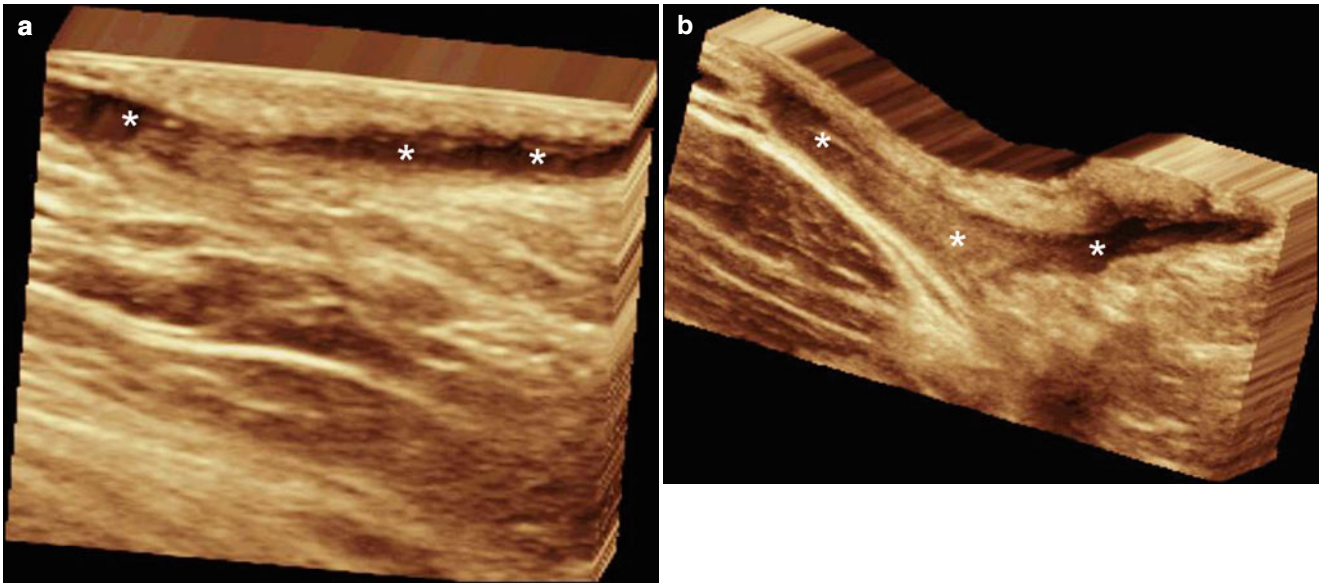

Fig. 4.44 (**a**, **b**). 3D of fistulous tracts (*) in hidradenitis suppurativa (5–8 s longitudinal view reconstructions)

4.2.14 Foreign Bodies

Foreign bodies are exogenous components that can be retained in the skin through many mechanisms commonly related to trauma. Occasionally, patients are not aware of the retained material but clinically they present with induration, erythema, and scarring. There are two main types of foreign bodies according to origin: organic (derived from living structures) such as splinters of wood or thorns of roses, or inert, also called synthetic, such as pieces of glass or metal.

Histology shows giant cells, macrophages, and inflammatory cells. Some foreign bodies such as wood, suture material, or glass are birefringent and can be identified using polarized light.

On sonography, foreign bodies appear as hyperechoic linear or band-like structures. Inert materials such as glass or metal usually show a posterior reverberance artifact. Commonly, there is hypoechoic granulomatous tissue surrounding the foreign body. Fluid collections in the vicinity such as hematomas or abscesses, or the involvement of deeper structures, can be ruled out. Occasionally, these foreign bodies may migrate and/or can be found far from the puncture wound level; therefore, it is suggested to examine a wide range of tissue. Sonography may prove their existence, assess the exact axis, location and measurements and also guide the removal. In an acute setting, the sonographer should avoid the contamination of the open wound with gel, therefore, the usage of sterile gel is recommended. In the presence of soft-tissue emphysema, a lateral approach to the wound or a water bath (when the lesional area is located in the distal arm or leg) can help [53–55] (Figs. 4.45, 4.46 and 4.47).

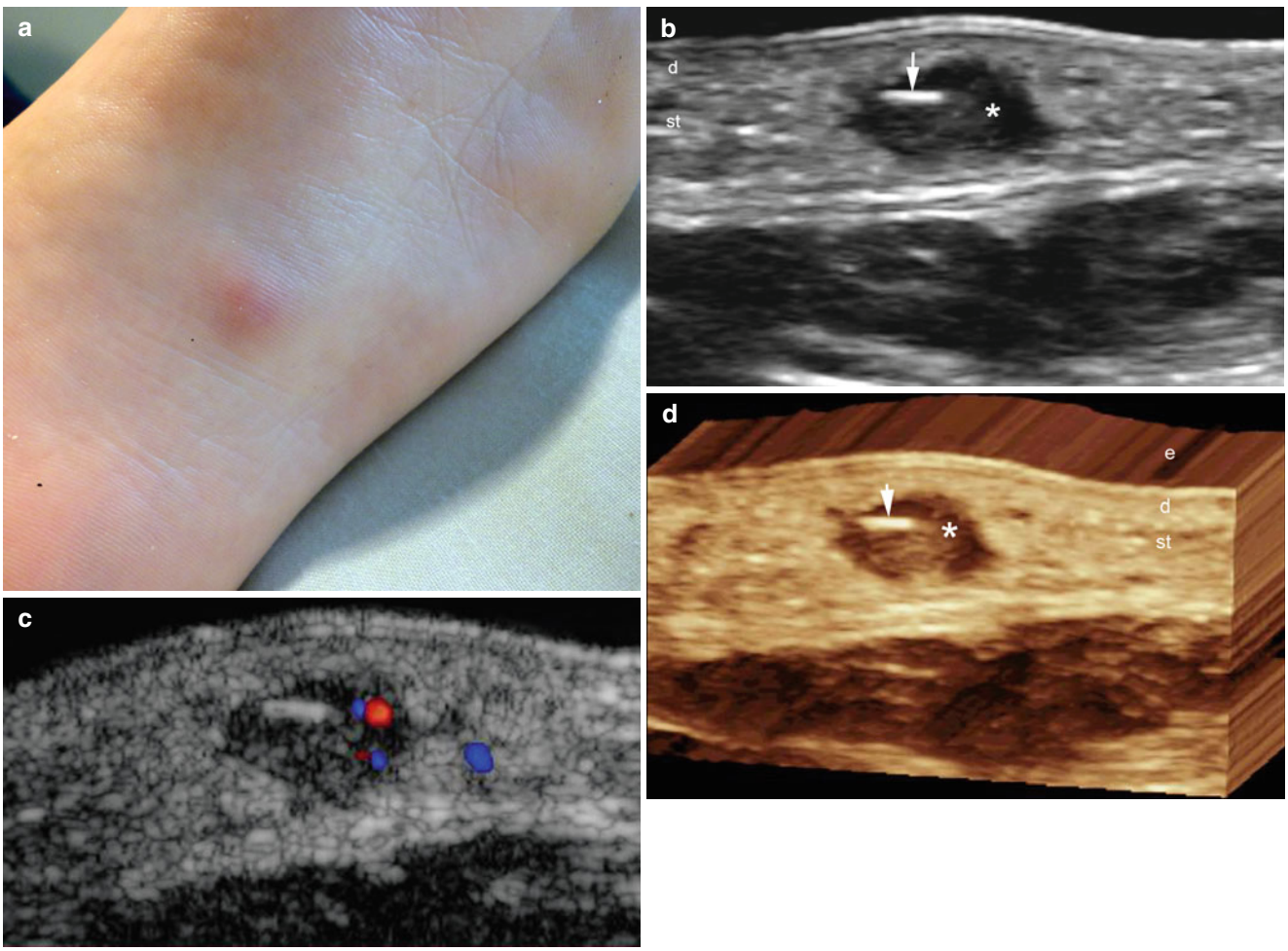

Fig. 4.45 (**a**–**d**) Organic foreign body. (**a**) Clinical image shows erythematous swelling in the medial aspect of the sole of the left foot. (**b**) Gray scale ultrasound image (longitudinal view) demonstrates hyperechoic line (*arrow*) in the subcutaneous tissue that corresponds to a fragment of a splinter of wood. Hypoechoic granulomatous tissue (*) surrounds the foreign body. Notice the bilaminar normal appearance of the plantar epidermis. (**c**) Color Doppler ultrasound image (transverse view) shows increased blood flow in the hypoechoic granulomatous tissue. (**d**) 3D reconstruction of the foreign body (5–8 s transverse view sweep). *Abbreviations*: *e* epidermis, *d* dermis, *st* subcutaneous tissue

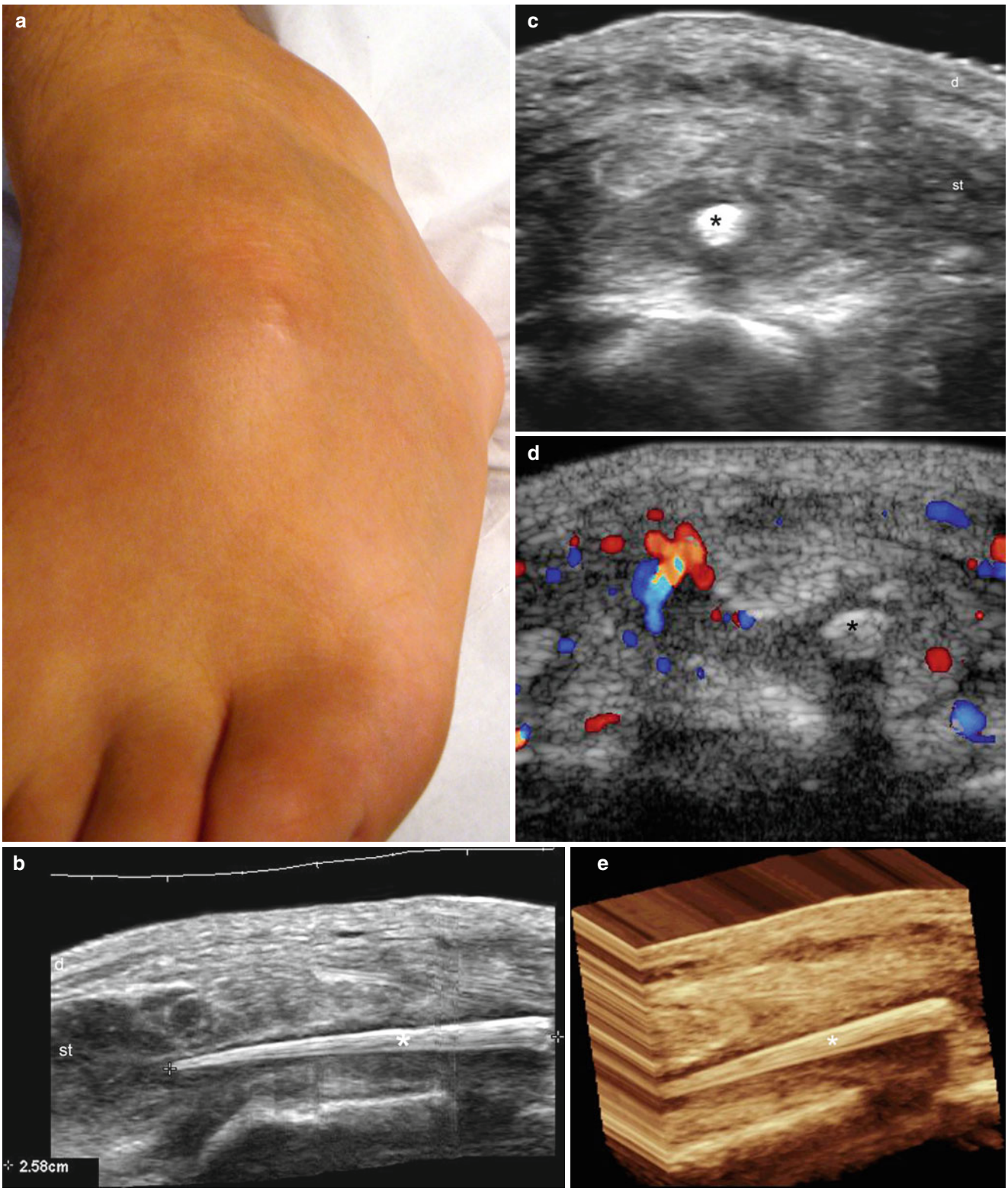

Fig. 4.46 (**a**–**e**) Organic foreign body. (**a**) Clinical image shows a swelling in the anterolateral aspect of the left foot. (**b**) Gray scale ultrasound image (longitudinal view) demonstrates a 2.58 cm, well defined, hyperechoic band (*) with tapering of its distal part, located in the subcutaneous tissue that corresponded to a fragment of a leaf of a palm tree. (**c**) Gray scale ultrasound image (transverse view) demonstrates the foreign body (*) and the surrounding hypoechoic granulomatous tissue in the periphery. (**d**) Color Doppler ultrasound image (transverse view) shows increased blood flow surrounding the foreign body. (**e**) 3D reconstruction of the foreign body (5–8 s longitudinal sweep). *Abbreviations*: *d* dermis, *st* subcutaneous tissue

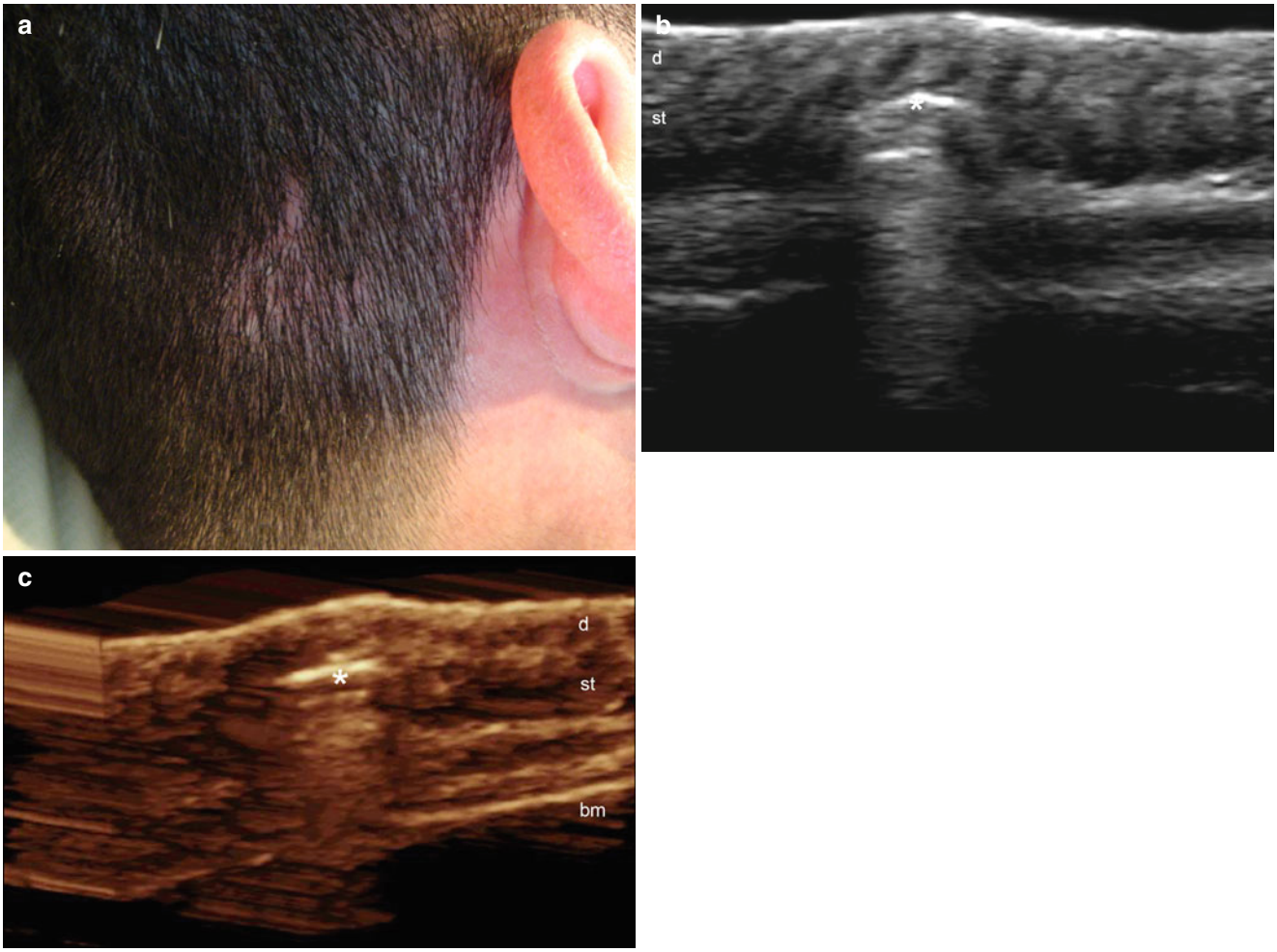

Fig. 4.47 (**a**–**c**) Inert foreign body. (**a**) Clinical image shows focal baldness and erythema in the right occipital region. (**b**) Gray scale ultrasound image (longitudinal view) demonstrates hyperechoic band (*) in the subcutaneous tissue that produces a posterior reverberance artifact that corresponded to a piece of glass. Notice the enlargement of the hair follicles superficially located and the compression of the superficial hair follicles performed by the foreign body. (**c**) 3D of the foreign body (5–8 s longitudinal view reconstruction). *Abbreviations*: *d* dermis, *st* subcutaneous tissue

References

1. Wortsman XC, Holm EA, Wulf HC, Jemec GB. Real-time spatial compound ultrasound imaging of skin. Skin Res Technol. 2004;10:23–31.
2. Hermann G, Gilbert MS, Abdelwahab IF. Hemophilia: evaluation of musculoskeletal involvement with CT, sonography, and MR imaging. AJR Am J Roentgenol. 1992;158:119–23.
3. Badauy CM, Gomes SS, Sant'Ana Filho M, Chies JA. Ehlers-Danlos syndrome (EDS) type IV: review of the literature. Clin Oral Investig. 2007;11:183–7.
4. Sidhu PS, Rich PM. Sonographic detection and characterization of musculoskeletal and subcutaneous tissue abnormalities in sickle cell disease. Br J Radiol. 1999;72:9–17.
5. Török L, Kirschner A, Ocsai H, Olasz K. Hematoma-like metastasis in melanoma. J Am Acad Dermatol. 2003;49:912–3.
6. Ebright JR, Pieper B. Skin and soft tissue infections in injection drug users. Infect Dis Clin North Am. 2002;16:697–712.
7. Latifi HR, Siegel MJ. Color Doppler flow imaging of pediatric soft tissue masses. J Ultrasound Med. 1994;13:165–9.
8. Noh JY, Cheong HJ, Song JY, Hong SJ, Myung JS, Choi WS, et al. Skin and soft tissue infections: experience over a five-year period and clinical usefulness of ultrasonography-guided gun biopsy-based culture. Scand J Infect Dis. 2011;43:870–6.
9. Naouri M, Samimi M, Atlan M, Perrodeau E, Vallin C, Zakine G, et al. High-resolution cutaneous ultrasonography to differentiate lipoedema from lymphoedema. Br J Dermatol. 2010;163:296–301.
10. Volikova AI, Edwards J, Stacey MC, Wallace HJ. High-frequency ultrasound measurement for assessing post-thrombotic syndrome and monitoring compression therapy in chronic venous disease. J Vasc Surg. 2009;50:820–5.
11. Wollina U, Abdel-Naser MB, Mani R. A review of the microcirculation in skin in patients with chronic venous insufficiency: the problem and the evidence available for therapeutic options. Int J Low Extrem Wounds. 2006;5:169–80.
12. Leu AJ, Leu HJ, Franzeck UK, Bollinger A. Microvascular changes in chronic venous insufficiency-a review. Cardiovasc Surg. 1995;3:237–45.
13. Meissner MH. Lower extremity venous anatomy. Semin Intervent Radiol. 2005;22:147–56.
14. Liu X, Jia X, Guo W, Xiong J, Zhang H, Liu M, et al. Ultrasound-guided foam sclerotherapy of the great saphenous vein with sapheno-femoral ligation compared to standard stripping: a prospective clinical study. Int Angiol. 2011;30:321–6.
15. Miteva M, Romanelli P, Kirsner RS. Lipodermatosclerosis. Dermatol Ther. 2010;23:375–88.
16. Kirsner RS, Pardes JB, Eaglstein WH, Falanga V. The clinical spectrum of lipodermatosclerosis. J Am Acad Dermatol. 1993;28:623–7.
17. Gniadecka M, Karlsmark T, Bertram A. Removal of dermal edema with class I and II compression stockings in patients with lipodermatosclerosis. J Am Acad Dermatol. 1998;39:966–70.
18. Chopra R, Chhabra S, Thami GP, Punia RP. Panniculitis: clinical overlap and the significance of biopsy findings. J Cutan Pathol. 2010;37:49–58.
19. Requena L, Yus ES. Panniculitis. Part I. Mostly septal panniculitis. J Am Acad Dermatol. 2001;45:163–83.
20. Requena L, Sánchez Yus E. Panniculitis. Part II. Mostly lobular panniculitis. J Am Acad Dermatol. 2001;45:325–61.
21. Avayú HE, Rodríguez AC, Wortsman CX, Corredoira SY, Serman VD, Strauch BG, et al. Newborn fat necrosis: case-report. Rev Chil Pediatr. 2009;80:60–4. Spanish.
22. Wortsman X, Gutierrez M, Saavedra T, Honeyman J. The role of ultrasound in rheumatic skin and nail lesions: a multi-specialist approach. Clin Rheumatol. 2011;30:739–48.
23. Cohen PR, Eliezri YD. Cutaneous odontogenic sinus simulating a basal cell carcinoma: case report and literature review. Plast Reconstr Surg. 1990;86:123–7.
24. Wortsman X, Wortsman J. Skin ultrasound, Chap. 9. In Dogra V, Gaitini D, editors. Musculoskeletal ultrasound with CT and MRI correlation,1st edn. Thieme, Stuttgart; 2010. p. 147–170.
25. Wortsman X, Sazunic I, Jemec GB. Sonography of plantar warts: role in diagnosis and treatment. J Ultrasound Med. 2009;28:787–93.
26. Wortsman X, Jemec GB, Sazunic I. Anatomical detection of inflammatory changes associated with plantar warts by ultrasound. Dermatology. 2010;220:213–7.
27. Johnson MA, Armstrong AW. Clinical and Histologic diagnostic guidelines for psoriasis: a critical review. Clin Rev Allergy Immunol. 2013;44:166–72.
28. Baran R. The burden of nail psoriasis: an introduction. Dermatology. 2010;221 Suppl 1:1–5.
29. Yamamoto T. Psoriatic arthritis: from a dermatological perspective. Eur J Dermatol. 2011;21:660–6.
30. Murphy M, Kerr P, Grant-Kels JM. The histopathologic spectrum of psoriasis. Clin Dermatol. 2007;25:524–8.
31. Gutierrez M, Wortsman X, Filippucci E, De Angelis R, Filosa G, Grassi W. High-frequency sonography in the evaluation of psoriasis: nail and skin involvement. J Ultrasound Med. 2009;28:1569–74.
32. Gutierrez M, De Angelis R, Bernardini ML, Filippucci E, Goteri G, Brandozzi G, et al. Clinical, power Doppler sonography and histological assessment of the psoriatic plaque: short-term monitoring in patients treated with etanercept. Br J Dermatol. 2011;164:33–7.
33. Kaeley GS. Review of the use of ultrasound for the diagnosis and monitoring of enthesitis in psoriatic arthritis. Curr Rheumatol Rep. 2011;13:338–45.
34. Fett N, Werth VP. Update on morphea: part I. Epidemiology, clinical presentation, and pathogenesis. J Am Acad Dermatol. 2011;64:217–28.
35. Wollina U, Buslau M, Heinig B, Petrov I, Unger E, Kyriopoulou E, et al. Disabling pansclerotic morphea of childhood poses a high risk of chronic ulceration of the skin and squamous cell carcinoma. Int J Low Extrem Wounds. 2007;6:291–8.
36. Li SC, Liebling MS, Haines KA. Ultrasonography is a sensitive tool for monitoring localized scleroderma. Rheumatology (Oxford). 2007;46:1316–9.
37. Li SC, Liebling MS. The use of Doppler ultrasound to evaluate lesions of localized scleroderma. Curr Rheumatol Rep. 2009;11:205–11.
38. Wortsman X, Wortsman J, Sazunic I, Carreño L. Activity assessment in morphea using color Doppler ultrasound. J Am Acad Dermatol. 2011;65:942–8.
39. Wenzel J, Zahn S, Tüting T. Pathogenesis of cutaneous lupus erythematosus: common and different features in distinct subsets. Lupus. 2010;19:1020–8.
40. Rothfield N, Sontheimer RD, Bernstein M. Lupus erythematosus: systemic and cutaneous manifestations. Clin Dermatol. 2006;24:348–62.
41. Tebbe B. Clinical course and prognosis of cutaneous lupus erythematosus. Clin Dermatol. 2004;22:121–4.
42. Delle Sedie A, Riente L, Filippucci E, et al. Ultrasound imaging for the rheumatologist. XV. Ultrasound imaging in vasculitis. Clin Exp Rheumatol. 2008;26:391–4.
43. Wortsman X. The traces of sound: taking the road to skin. Curr Rheumatol Rev. 2011;3:231–8.

44. Kao L, Chung L, Fiorentino DF. Pathogenesis of dermatomyositis: role of cytokines and interferon. Curr Rheumatol Rep. 2011;13:225–32.
45. Koler RA, Montemarano A. Dermatomyositis. Am Fam Physician. 2001;1(64):1565–72.
46. Weber MA. Ultrasound in the inflammatory myopathies. Ann N Y Acad Sci. 2009;1154:159–70.
47. Stonecipher MR, Jorizzo JL, Monu J, Walker F, Sutej PG. Dermatomyositis with normal muscle enzyme concentrations. A single-blind study of the diagnostic value of magnetic resonance imaging and ultrasound. Arch Dermatol. 1994;130(10):1294–9.
48. Jemec GB. Clinical practice. Hidradenitis suppurativa. N Engl J Med. 2012;366:158–64.
49. Layton A. Pathology of Hidradenitis Suppurativa. In: Jemec GBE, Revuz J, Leyden J, editors. Hidradenitis Suppurativa. Berlin: Springer- Verlag; 2006. p. 25–33.
50. Wortsman X, Jemec GB. Real-time compound imaging ultrasound of hidradenitis suppurativa. Dermatol Surg. 2007;33:1340–2.
51. Wortsman X, Revuz J, Jemec GB. Lymph nodes in hidradenitis suppurativa. Dermatology. 2009;219:22–4.
52. Kelekis NL, Efstathopoulos E, Balanika A, Spyridopoulos TN, Pelekanou A, Kanni T, et al. Ultrasound aids in diagnosis and severity assessment of hidradenitis suppurativa. Br J Dermatol. 2010;162:1400–2.
53. Halaas GW. Management of foreign bodies in the skin. Am Fam Physician. 2007;76:683–8.
54. Valle M, Zamorani MP. Skin and subcutaneous tissue. In: Bianchi S, Martinoli C, editors. Ultrasound of musculoskeletal system. Berlin: Springer- Verlag; 2007. p. 27–31.
55. Wortsman X. Common applications of dermatologic sonography. J Ultrasound Med. 2012;31:97–111.